2017

Understanding the Role of Runx2 in a Breast Cancer Progression Cell Model

Alexandra Ojemann
University of Vermont

UNDERSTANDING THE ROLE OF RUNX2 IN A BREAST CANCER PROGRESSION CELL MODEL

A Thesis Presented

by

Alexandra Ojemann

to

The Faculty of the Graduate College

of

The University of Vermont

In Partial Fulfillment of the Requirements
for the Degree of Master of Science
Specializing in Biochemistry

May, 2017

Defense Date: March 20, 2017
Thesis Examination Committee:

Janet Stein, Ph.D., Advisor
Eyal Amiel, Ph.D., Chairperson
Stephen Everse, Ph.D.
Cynthia J. Forehand, Ph.D., Dean of the Graduate College

ABSTRACT

Runx2 is a transcription factor required for bone formation and osteoblastic differentiation during normal development and is implicated in metastatic disease during breast cancer progression. Runx2 is highly expressed in many metastatic breast cancers and breast cancer cell lines Knockdown of Runx2 in various breast cancer cell lines restores epithelial characteristics and reduces proliferation, migration, and invasion. However, the role of Runx2 in breast cancer progression from early to late stages is not well understood. The MCF10A derived breast cancer progression model provides the opportunity to study the role of Runx2 in a series of cell lines that progress from nearly normal, with low Runx2 levels, to highly metastatic and aggressive, with much higher Runx2 levels. To address if removal of Runx2 affects gene expression and what pathways it may influence, specifically focused on breast cancer progression, we knocked down Runx2 using an shRNA lentivirus. Depletion of Runx2 inhibits the expression of mesenchymal markers including N-cadherin, Fibronectin, and Vimentin. Despite this finding, functional characteristics including proliferation, migration, and invasion were minimally affected. Possible reasons for the difference in results compared to other cell systems are discussed. As an alternative approach, we have generated stable, inducible cell lines using CRISPRi dCas9-KRAB to target Runx2 and in the future will investigate the effects of Runx2 knockdown in these cells.

ACKNOWLEDGEMENTS

I would like to thank the entire Stein/Lian lab for allowing me to work alongside them all year: Gary Stein, Janet Stein, Jane Lian, Prachi Ghule, Kirsten Tracy, Coralee Tye, Terri Messier, Deli Hong, Andy Fritz, Mark Fitzgerald, Natalie Page, Mingu Kang, Kaleem Zaidi, Jonathan Gordon, Kristiaan Finstad, Taylor Putnam, Nicholas Farina, Jessica Heath, and Joseph Boyd. I would like to thank Janet Stein for her work as my advisor, all of her support, and helpful discussion and feedback. Special thanks to my mentor Prachi Ghule who guided me through this project, helped me develop the skills I needed, and didn't run away when she saw me coming to ask her my 75th question of the day!

Also pertinent to the successful completion of this project was the UVM AGTC staff as well as Roxanna del Rio-Guerra, who put in long hours sorting the cells used in this project.

I would also like to thank my thesis committee for their time and efforts: Eyal Amiel (Chairperson), Stephen Everse, and Janet Stein (Advisor).

Finally, thank you to my friends, family, fiancé, and my horse Sunny for their support during this past year.

Funding from NIH-NCI P01CA082834

TABLE OF CONTENTS

LIST OF TABLES

LIST OF FIGURES

Figure Page

CHAPTER 1: INTRODUCTION

1.1 Runx

Runt-related transcription factors, or Runx, were identified in three different organisms. First, in *Drosophila melanogaster* as the segmentation gene Runt, then in acute myeloid leukemia patients as a chromosome translocation, and lastly in the polyoma-virus enhancer binding protein 2 (Ito et al., 2015). Mammals have three Runx proteins, Runx1, Runx2, and Runx3 that are expressed in a tissue-dependent manner (Ito et al., 2015). The three closely related genes likely emerged from a triplication mutation, implied by a 128 amino acid conserved runt DNA binding domain (Blyth, Cameron, & Neil, 2005). Each Runx gene is involved in a developmental pathway and is also associated with different types of cancer. Runx1 mutations are associated with human leukemia, whereas the overexpression of Runx2 in breast and prostate cancer cells leads to metastasis to bone, and inactivation of Runx3 contributes to cancer pathogenesis and is common in human gastric carcinomas (Blyth et al., 2005; Ito et al., 2015). Runx1 has a role in hematopoiesis, Runx2 in bone development, and Runx3 in gastrointestinal/neuronal development (Owens et al., 2014).

Runx proteins share common features, including a common DNA binding domain called runt, as well as two promoters (Figure 1) (Levanon & Groner, 2004; Vimalraj, Arumugam, Miranda, & Selvamurugan, 2015). They all bind the same DNA motif and use common transcriptional modulators (Levanon & Groner, 2004). Runx factors form a heterodimer with a co-transcription factor, CBFβ, which enables the recognition of the consensus sequence PyGPyGGTPy in the Runx targets (Vimalraj et al., 2015). Also

conserved is a CpG island at the C-terminus of each of the Runx genes (Levanon & Groner, 2004). Modifications to these CpG islands could affect the activities of the Runx genes and their expression. For example, a CpG island in Runx3 promoter 2 is hypermethylated in gastric cancer, but in promoter 1, where another CpG island is located, lack of methylation occurs in T cell lymphomas (Levanon & Groner, 2004).

In normal cells, Runx proteins are conserved regulators of cell fate. Runx factors contribute to regulation of gene expression as part of a core binding factor (CBF) complex. This Runx2-CBF complex regulates expression of many genes, including those that are related to cancer in both tumor suppressor and oncogenic pathways (Blyth et al., 2005).

Runx1 acts as a tumor suppressor in breast cancer (Chimge & Frenkel, 2013). It is the predominant Runx protein expressed in breast epithelial cells and was found to be mutated in many different patient samples in various breast cancer studies (Chimge & Frenkel, 2013). Loss of Runx1 in MCF7 breast cancer cells and MCF10A normal-like breast epithelial cells promotes an epithelial to mesenchymal transition (EMT) (Hong et al., 2017). EMT is an important event in cancer progression, allowing cancer cells to develop metastatic potential (Hong et al., 2017). One mechanism through which this occurs is that Runx1 directly upregulates the epithelial marker, E-cadherin, preventing the cells from losing epithelial characteristics. Further evidence to support this result is that upon depletion of Runx1 in MCF10A cells, E-cadherin levels decrease (Hong et al., 2017).

Runx3 appears to act as a tumor suppressor in some cancers, as overexpression of Runx3 results in the inhibition of growth in carcinoma cell lines (Blyth et al., 2005). In

patient samples, Runx3 levels seem to decrease as breast cancer progresses and furthermore, higher levels of Runx3 are associated with a more favorable prognosis (Chimge & Frenkel, 2013). One cause of Runx3 deregulation in breast cancer could be estrogen signaling. There is a positive relationship between estrogen levels and risk of breast cancer (Colditz, 1998). Treatment with Estradiol, a type of estrogen, results in hypermethylation of the promoter, preventing transcription of Runx3 (Chimge & Frenkel, 2013).

Runx2 has two promoters, which leads to the production of two isoforms with 521 and 507 amino acids, respectively (Vimalraj et al., 2015). Runx2 is required for normal mammary alveolar development during late pregnancy and for the specification of alveolar cell maturation (Owens et al., 2014). It also functions as a regulator of osteoblastic differentiation, skeletal morphogenesis, and stem cell differentiation into osteogenic lineages (Vimalraj et al., 2015). Runx2 levels have been shown to remain constant through adulthood and early to mid-pregnancy in mice mammary tissues, however levels drop significantly towards the end of pregnancy and throughout lactation (Owens et al., 2014).

Runx2 is also required for bone formation, and Runx2 knockout mice die at birth (Choi et al., 2001). Deletions at the C terminus are particularly detrimental; causing mice with this c terminal deletion to die in utero, versus Runx2 null mice, which die at birth (Choi et al., 2001). Significant development problems occur when even one copy of Runx2 is missing due to haploinsufficiency (Choi et al., 2001).

Figure 1: Homology between Runx1, 2, and 3 (Ito et al., 2015)**.** Each protein has a Runt domain, which is the DNA binding domain, an activation domain (AD), an inhibitory domain (ID), and a VWRPY domain, which interacts with the co-repressors.

Runx2 is involved in breast cancer metastasis. In *in vitro* studies, Runx2 has proven to be a tumor promoter in most cases. It upregulates genes involved in cellular movement and cytoskeleton remodeling (Baniwal et al., 2010). Runx2 also activates matrix metalloproteases (MMP) 9 and 13, osteopontin, vascular endothelial growth factor (VEGF), and the bone resorbing factors parathyroid hormone-related protein (PTHrP) and interleukin-8 (IL-8) in MDA-MB-231 and MCF7 breast cancer cell lines (Akech et al., 2010). Runx2 overexpression has been shown to cause aberrant proliferation and inhibition of apoptosis in normal mammary epithelial cells (Owens et al., 2014). In prostate cancer, Runx2 prevents apoptosis by stimulating the expression of Bcl2 and Survivin (Chimge & Frenkel, 2013). Overexpression of Runx2 also drives EMT-like changes in normal mammary epithelial cells and may also have a role in breast cancer metastasis to bone (Owens et al., 2014). Studies have shown that deletion of Runx2 in mammary epithelial cells in mice is associated with increased survival and reduced cell proliferation of basal breast cancer cells (Owens et al., 2014).

1.2 Epithelial to Mesenchymal Transition

The epithelial to mesenchymal transition occurs normally during embryogenesis and is a process in which epithelial cells change their shape and behavior (Mendez, Kojima, & Goldman, 2010). Epithelial cells lose polarity and attachment to neighboring cells, as well as basement membranes, and become flattened and elongated and change the composition of cytoskeletal components, upregulating vimentin and N-cadherin, while down regulating other types of cytoskeletal proteins such as E-cadherin (Mendez et al., 2010). These changes allow the cell to become motile and acquire an invasive phenotype (Lamouille, Xu, & Derynck, 2014). EMT also occurs during wound healing and tumorigenesis (Lamouille et al., 2014). The first step is usually the loss of cell-cell junctions, which normally help with the barrier function of epithelial cells. Next is the reorganization of the actin cytoskeleton to allow for elongation and direction-specific movement. Projections also develop and protrude out of the cell, acting as sensory organs (Lamouille et al., 2014). Other actin-rich protrusions produce chemicals that help degrade the extracellular matrix. Loss of normal cell polarity and the development of front-rear polarity also occurs at this point (Lamouille et al., 2014). Next, changes in protein expression are elicited. E-cadherin, a typical epithelial marker is downregulated and N-cadherin, a mesenchymal protein, is upregulated (Lamouille et al., 2014). Various transcription factors aside from Runx2 including SNAIL, TWIST, and ZEB are also involved in the control of expression of genes that regulate the EMT process (Lamouille et al., 2014).

Tumor cell metastasis occurs as EMT is completed and cells become detached from the original tumor. MMP 1 is expressed and is necessary for tumor cell invasion into bone, because it is a collagenase, and can dissolve bone (Kozlow & Guise, 2005). Tumor cells must extravasate from the original tumor site and enter systemic circulation (Kozlow & Guise, 2005). This can be accomplished by making new blood vessels in a process known as angiogenesis (Kozlow & Guise, 2005). Bone secretes chemicals that attract the tumor cells, such as SDF-1, which binds to the CXCR4 receptor on the tumor cells. Tumor cells then become trapped in bone marrow and must reach and adhere to the endosteal surface in order to survive (Kozlow & Guise, 2005).

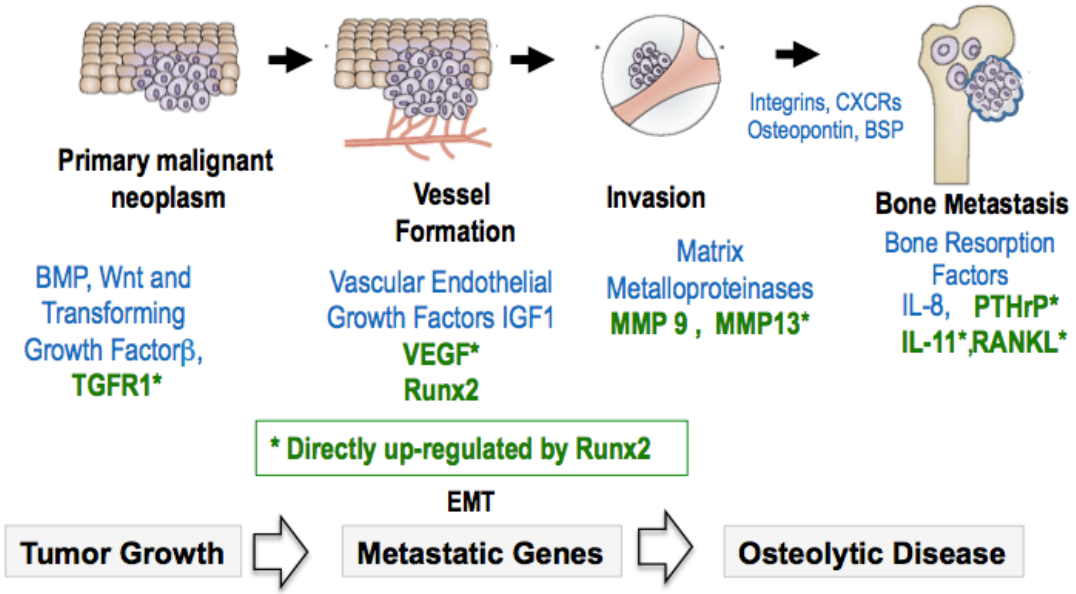

Figure 2: Genes controlled by Runx2 involved in EMT. Primary tumor cells undergo changes in gene expression profiles to be able to metastasize and grow in bone. Factors including VEGF, MMPs, and PTHrP mediate some of the changes necessary for cellular processes involved in metastatic transformation, and are regulated directly by Runx2 (Pratap et al., 2006).

1.3 Role of Runx2 in EMT and Metastasis

Runx2 is a transcription factor that regulates many genes that control the EMT process (Figure 2) (Pratap et al., 2006). Runx2 is implicated in breast cancer metastasis to bone causing osteolytic disease. *In* vitro experiments show that knockdown of Runx2 inhibits the ability of the cancer cells to interact with bone (Barnes et al., 2004). Furthermore, introducing mutant Runx2 in MDA-MB-231 breast cancer cells has been shown to cause a reversion to more normal breast tissue, and reduced proliferation (Pratap et al., 2009). Downstream targets of Runx2 have been shown to increase within many breast cancer cell lines where Runx2 is upregulated (Pratap et al., 2005). VEGF is a proangiogenic factor and is overexpressed during EMT (Gonzalez-Moreno et al., 2010). In prostate cancer cell lines, overexpression of VEGF leads to increased vascularization and tumorigenic capabilities (Gonzalez-Moreno et al., 2010). Other targets of Runx2 include epithelial markers such as E-cadherin, which decreases during EMT, and mesenchymal markers such as N-cadherin and Vimentin, which increase during EMT (Gonzalez-Moreno et al., 2010). N-cadherin allows cells to seek other cells expressing N-cadherin and promotes weaker interactions than does E-cadherin, allowing cells to remain motile and have invasive properties (Lamouille et al., 2014). Vimentin is also upregulated, while another type of intermediate filament, cytokeratin, is downregulated. Vimentin directs E-cadherin towards the cell membrane and interacts with motor proteins to help with cell motility (Lamouille et al., 2014). Expression or repression of various integrins that allow the cell to receive signals occurs during EMT, concordantly with MMP2 and 9 expression. MMP2 and 9 assist with extracellular matrix degradation, invasion, and further loss of cell-cell junctions (Lamouille et al., 2014). These changes allow the cell to be able to migrate from its original location and survive in a new

location. As shown in Figure 2, Runx2 is a direct mediator of many of the proteins involved in EMT, and the increased Runx2 levels in breast cancer cells compared to normal breast epithelial cells help to activate EMT to promote breast cancer progression (Pratap et al., 2006).

1.4 Breast Cancer Prevalence and Role of Runx2 in Metastasis

Breast cancer is the most commonly diagnosed cancer in women and the second leading cause of cancer-related deaths in women (DeSantis, Ma, Bryan, & Jemal, 2014). Metastasis of breast cancer cells is the cause of the most deaths associated with breast cancer because after breast cancer metastasizes to bone, it becomes incurable (Kozlow & Guise, 2005; Taylor, Sossey-Alaoui, Thompson, Danielpour, & Schiemann, 2013). In patients with advanced stages of breast cancer, 80% develop bone metastases, causing hypercalcemia, bone pain and fractures, and increased morbidity and mortality (Kozlow & Guise, 2005). Five-year survival drops from 98% to 23% when breast cancer becomes metastatic (Taylor et al., 2013). Another side effect of bone metastasis is cachexia, or muscle and fat wasting, which leads to skeletal related problems and events, and limits 2-year survival to 50% (Kozlow & Guise, 2005). Bone marrow suppression leading to leukopenia can also occur (Kozlow & Guise, 2005).

Certain cancers have a tendency to metastasize to bone, including breast and prostate cancer (Guise, 2002). When metastasis to bone does occur, the survival of the cancer cells in the bone is mediated by cancer cell-bone cell interactions (Guise, 2002). These interactions alter the bone microenvironment, allowing the cancer cell to survive, and creating what is known as the “vicious cycle” (Guise, 2002). The vicious cycle

occurs by osteoclast-mediated osteolytic bone destruction. PTHrP, the expression of which is controlled by Runx2, activates osteoclasts and results in increased osteoclast bone resorbing activities. Treatment with anti-PTHrP antibody decreases osteolytic bone destruction and inhibits the formation of bone metastases (Guise, 2002). TGFβ is stored in the bone matrix and is released upon osteoclast bone resorption. TGFβ also induces cancer cells to produce PTHrP. In breast cancer cell lines with mutant TGFβ receptors, PTHrP levels were decreased and bone metastasis growth slowed (Guise, 2002). PTHrP release can also be induced by high levels of extracellular calcium, which occurs during the vicious cycle (Guise, 2002). PTHrP also causes the increased expression of RANKL on osteoblasts, which is the activating receptor for osteoclasts (Kozlow & Guise, 2005).

Although the role of Runx2 in metastasis of breast cancer has been studied, the mechanism of regulation remains unclear, especially in early stage breast cancer. The mechanisms by which Runx2 enables metastasis to bone are important in understanding how breast cancer cells are able to survive in bone (Pratap et al., 2006). An increase in Runx2 expression allows breast cancer cells to behave more like osteoblasts, which leads to osteomimicry (Barnes et al., 2004). Osteomimicry is what helps breast cancer cells home to bone, making Runx2 a potential target for therapy (Barnes et al., 2004).

1.5 Breast Cancer Progression Model Cell Lines

The MCF10A cell line is a normal-like breast epithelial cell line that was transformed to generate a progression model to study breast cancers. The MCF10A parental cell line was isolated from benign breast tissue from a woman with fibrocystic

disease (Santner et al., 2001). MCF10A cells are considered normal because they do not invade or form tumors in immunodeficient mice (So, 2014).

MCF10A cells were transduced with T24 c-Ha-ras oncogene and then passaged through a mouse, generating the MCF10AT cells. The MCF10AT cells persist in small nodules and periodically form carcinomas when injected into mice (Dawson, Wolman, Tait, Heppner, & Miller, 1996). Cells from one of these carcinomas were grown in culture, generating the MCF10AT1 cell line (Dawson et al., 1996). MCF10AT1 cells are non-metastatic, premalignant cells (Santner et al., 2001).

MCF10CA1a are fully malignant, metastatic cells that are derived from MCF10AT cells (Santner et al., 2001). MCF10CA1a cells are the most aggressive cell line in the MCF10A series, with 100% transformation capacity in immunodeficient mice (Santner et al., 2001) (So, 2014). To develop the cell line, MCF10AT cells were injected into nude-beige mice. Cells that went on to produce carcinomas were cultured and cloned. One of the clones was used to create a second-generation xenograft. Subsequently, third and fourth generation tumors were created. These tumors were digested and then the cells injected into mice. The resulting cells that were isolated constitute the MCF10CA1a cell line and rapidly form tumors 100% of the time upon injection into mice, without evidence of a precursor stage (Santner et al., 2001). These three cell lines, MCF10A, MCF10AT1, and MCF10CA1a serve as a model to study various aspects in the biology of breast cancer progression (Santner et al., 2001). Runx2 levels in these cells increase as the cells transition from normal to cancerous (Figure 3).

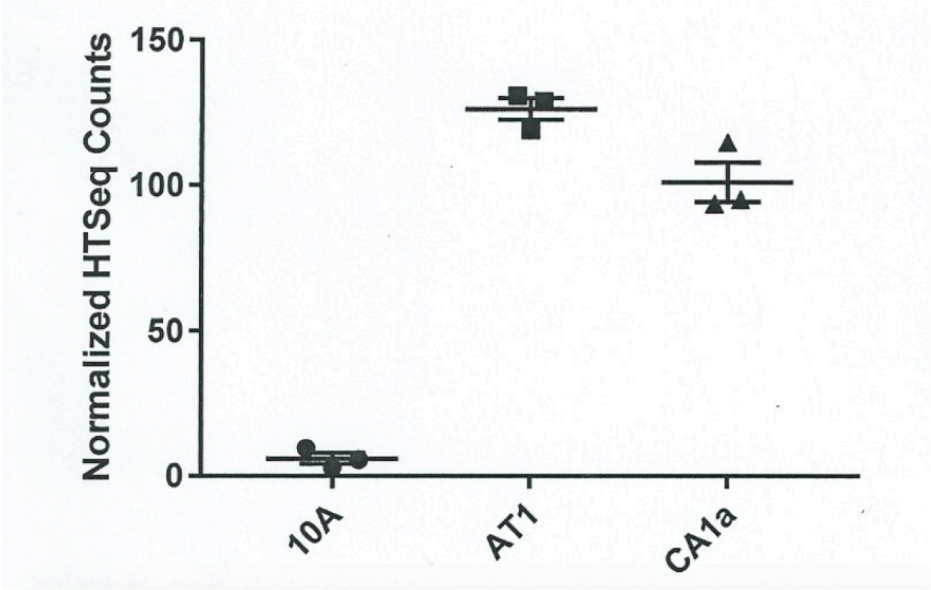

Figure 3: Runx2 mRNA levels in the MCF10A series. The MCF10A series were subject to global RNA sequencing using next generation sequencing. There is an increase in the Runx2 levels, as shown by the Normalized HTSeq Counts, as cells go from the normal MCF10A cells to the cancerous MCF10AT1 and MCF10CA1a cells.

1.6 Experimental Strategy

We used MCF10CA1a and MCF10AT1 cell lines to investigate the effects of Runx2 knockdown using both CRISPRi and short hairpin RNA-Runx2 systems. Stable cell lines expressing the shRunx2 and the dCas9/guide RNA were generated. In the shRunx2 cells, GFP was used to select for cells with similar, medium amounts of shRNA expression. For CRISPRi, Geneticin, also known as G418, and Puromycin were used as a selection for integration of the dCas9 and guide RNAs, respectively. Using these stable cell lines, levels of Runx2 itself and its targets, as mentioned by Pratap et. al, 2005, including osteocalcin, osteopontin, PTHrP, VEGF, IL-8, Survivin, E-cadherin, Vimentin, and N-cadherin were measured to characterize these Runx2 knockdown cells via real

time PCR and Western blotting. Western blotting was used as a definitive method to check Runx2 knockdown efficiency and confirm the effect of Runx2 knockdown on the proteins listed above. RNA sequencing was performed on these cells to investigate global changes in gene expression.

Due to the known role of Runx2 in regulating invasion and migration in MDA-MB-231 cells (Pratap et al., 2009), functional assays were performed that measure cell proliferation, migration, and invasion. We performed a proliferation assay to measure cell proliferation each day, a scratch (wound healing) assay to assess motility of cells, as well cell invasion and migration assays using Transwell chambers with or without Matrigel. These assays were done in both the MCF10CA1a and MCF10AT1 cells expressing shRunx2, and the control cells were infected with empty vector (EV) plasmid containing lentivirus.

Although the role of Runx2 in breast cancer metastasis has been studied, the role of Runx2 in early cancer events remains unclear. One of the aims of our project is to begin to understand the consequences of Runx2 knockdown on Runx2 target genes in less aggressive breast cancers, represented by MCF10AT1. The MCF10A cell lines allow us to study the global effects of Runx2 knockdown in both aggressive (MCF10CA1a) and non-metastatic cells (MCF10AT1)- a breast cancer progression model.

CHAPTER 2: MATERIALS AND METHODS

2.1 Cell Culture

MCF10CA1a cells were maintained in DMEM (Corning CellGro), 5% horse serum (Gibco 16050), 1% Penicillin streptomycin (Gibco Life Technologies), and 1% L-glutamine (Gibco Life Technologies) at 37°C. MCF10AT1 cells were maintained in DMEM (Corning CellGro), 5% horse serum (Gibco 16050), 1% Penicillin streptomycin (Gibco Life Technologies), 1% L-glutamine (Gibco Life Technologies) 10 μg/mL Human insulin (Sigma I-1882), 20 ng/mL hEGF (Gibco Life Technologies), 100 ng/mL Cholera Toxin (Sigma C-8052), and 0.5 μg/mL Hydrocortisone (Sigma H-0888) at 37 °C. To subculture the cells, 0.25% trypsin was diluted 1:10, and added to cells for 20 minutes, and cells were replated 1:10.

HEK-293-FT cells were grown in DMEM (Corning CellGro), 10% Fetal Bovine Serum (Atlanta), 1% Penicillin streptomycin, 1% L-glutamine, 1% MEM Non-essential amino acid solution (Gibco Life Technologies), and 500 μg/mL Geneticin (Sigma-Aldrich).

To freeze cells, Bambanker Cryopreservation Medium (Wako Pure Chemical 302-14681) was used to resuspend pelleted cells at a density between 2 and 10 million cells per mL. One milliliter of solution was dispensed into each cryovial. Cryovials were frozen at -80°C in a container filled with isopropanol and stored at -80°C.

2.2 Lentiviral Transduction

Lentiviruses are an effective vector for altering gene expression in mammalian cells. Lentiviruses can be used to carry shRNA into cells in order to silence gene

expression, in a process of posttranscriptional gene modification known as RNA interference (Van den Haute, Eggermont, Nuttin, Debyser, & Baekelandt, 2003). RNA interference was designed as a faster and cheaper alternative to genetic knockouts that could be used in a larger variety of organisms (Stewart et al., 2003). The lentivirus is used to deliver shRNA that will knock down expression of a specific gene (Rubinson et al., 2003). When the lentivirus enters the cell, the shRNAs are cleaved by Dicer, generating small dsRNAs that are able to induce knockdown of the target gene (Stewart et al., 2003). One advantage of the lentiviral system is that it can be used in non-dividing cells (Stewart et al., 2003). Another advantage is that silencing of the genes delivered by lentiviral vectors does not occur during development, meaning embryonic stem cells can be transduced (Rubinson et al., 2003). The shRNA can also be selected for to generate and maintain stable cell lines (Rubinson et al., 2003).

Stable cell lines expressing empty vector or shRunx2 were generated as follows: MCF10CA1a cells, passage 34, were infected with Runx2 PLVTHM Sh 4/4 lentivirus or PwtsI empty vector (EV) (Figure 4), as described in Afzal et al., 2005. PLVTHM vector used in this study co-expresses green fluorescent protein (GFP) along with the shRNA or EV, and can be used as a selection marker. Cells were plated at $3x10^5$ cells/well on a 6-well plate in 2 mL of the MCF10CA1a or MCF10AT1 media described above. Cells were cultured for 24 hours to about 40% confluency before 100 or 150 μL of virus with 4 μg/mL polybrene were added to each well. After 24 hours the medium was replaced. Forty-eight hours after the initial plating, cells were trypsinized and split into 100 mm plates. MCF10AT1 cells were infected the same way; however, it is necessary to plate these cells at a lower initial density since they grow much more rapidly. This infection

was done in three separate instances for both MCF10CA1a and MCF10AT1 cell lines to create three biological replicates per line. After passage 3 post-infection, live cells were sorted using flow cytometry, as described in the next section.

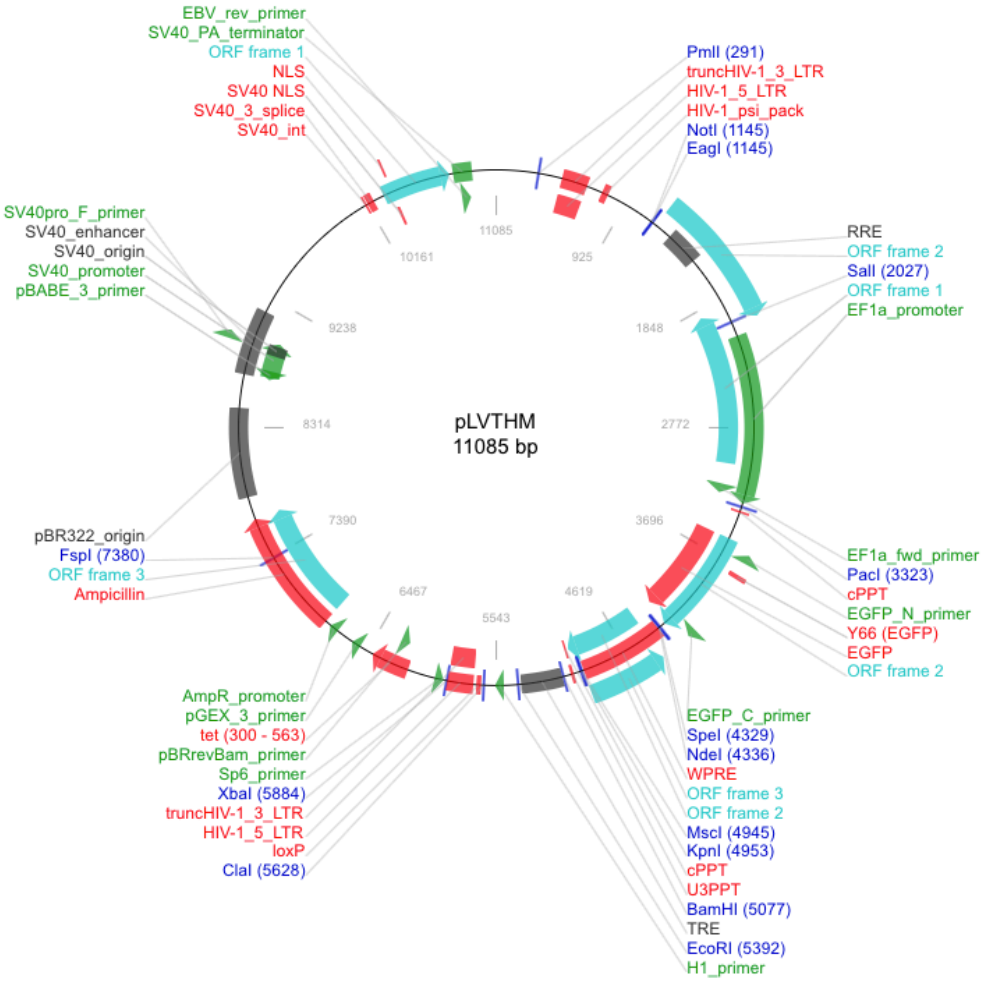

Figure 4: Lentiviral vector used for generation of shRNA against Runx2 (Wiznerowicz & Trono, 2003). The EV is the same vector without the shRNA against Runx2.

2.3 Flow Cytometry for Live Cell Sorting

After infection, cells were sorted for GFP using Fluorescence-Activated Cell Sorting (FACS). FACS is a type of flow cytometry that analyzes and sorts live cells based on expression of fluorescently tagged proteins (Figure 5) (Herzenberg et al., 2002). Cells were collected via trypsinization, washed with PBS, filtered through 100 micron cell strainers to avoid clumps, and resuspended in 1% horse serum DMEM. Cells were brought to the University of Vermont Flow Cytometry and Cell Sorting Facility where they underwent a one-way sort to select cells expressing medium levels of GFP on a BD FACS AriaII machine. The BD FACS AriaII can perform up to four-way sorting, detect up to 13 fluorescent signals, as well as forward and side scatter, at three different nozzle pressures. Only the cells expressing GFP at intermediate levels were collected, and the high and low expressing cells were not used (Figure 5). To determine optimal GFP concentration for cell sorting, we first collected both high and low GFP expressing cells. We observed broad variation and inconsistent Runx2 knockdown within samples; therefore we decided to select cells expressing medium levels of GFP that showed minimal variability. A purity check was performed on the samples after sorting to ensure that only the medium GFP expressing cells were collected. After collection, cells were plated at a density between 0.8-2 million cells per 100 mm plate in complete media.

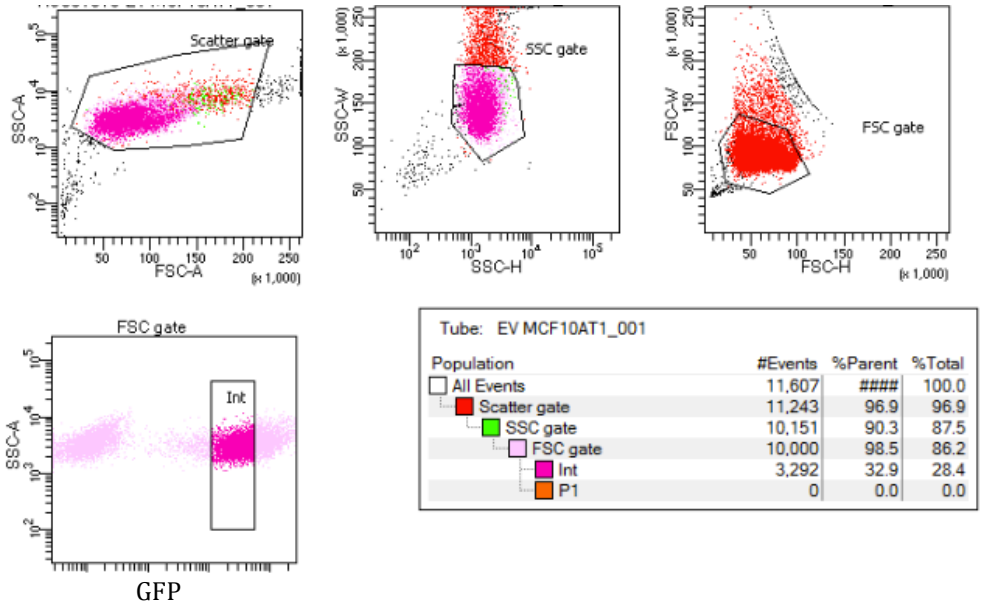

Figure 5: Cell Sorting and Gating Strategy after transduction with lentivirus. The SSC and FSC, or side scatter and forward scatter gates show that population of cells based on size parameters. In these gates, cells are distinguished from debris based on size. The GFP graph shows the population of cells we collected based on intermediate GFP expression.

2.4 CRISPR/Cas9 System

Clustered Regularly Interspaced Short Palindromic Repeats (CRISPR) is a bacterial immune system that can be utilized for genome engineering. There are two critical components of the CRIPSR system, the guide RNA (gRNA), which binds to a specific sequence and helps to localize the second component, CRISPR-associated endonuclease, Cas9 (Larson et al., 2013). CRIPSR interference, or CRIPSRi uses a catalytically dead version of Cas9, lacking endonuclease activity, called dCas9 with an

attached KRAB repressor domain (Larson et al., 2013). The dCas9 gets stuck on the mRNA while the KRAB domain represses translation (Larson et al., 2013). CRISPRi has many advantages over traditional gene editing in that it is inducible/reversible and is simple and inexpensive because it requires gRNA sequences to be only 20 nucleotides long (Larson et al., 2013). Various sites within the gene can also be targeted with dCas9, allowing for specific regulation of gene expression so that translation or translation initiation can be effected (Larson et al., 2013). Off-target effects as seen with RNAi and the expensive nature of Zinc-finger proteins are mostly avoided when using CRISPRi (Larson et al., 2013). Limitations include the necessity for a protospacer adjacent motif (PAM) sequence of NGG when targeting the dCas9 to a location in the genome. There are, however, other PAM sequences that are becoming available for use with the CRISPRi system (Larson et al., 2013). Off target effects can be seen in large genomes due to the short nature of the CRISPRi targeting, but longer PAMs could prevent this from occurring (Larson et al., 2013).

Guide RNAs tagging both promoters of the RUNX2 gene were designed using Benchling software (Figure 7) (https://benchling.com). Primers were annealed using ligation buffer and T4 Polynucleotide Kinase (New England Biolabs). Primers were diluted from 100μM 1:250. Primers were then ligated into the LentiGuide-Puro backbone (Addgene) with FastDigest reagents (Thermo Fisher). DNA was then treated with PlasmidSafe Buffer and DNase (Illumina). Plasmids were then transformed into One Shot™ Stbl3™ Chemically Competent *E. coli*. Colonies were selected and grown in LB-Amp broth overnight. Minipreps were performed on these colonies using the Zyppy™ Plasmid Miniprep kit (Zymo Research), and DNA was sequenced. Selected DNA was

transformed into One Shot™ Stbl3™ Chemically Competent *E. coli* (Invitrogen) and resequenced to ensure recombination did not occur. Midi preps were prepared from these cultures and DNA was isolated using the ZymoPURE™ Plasmid Midiprep kit (Zymo Research).

Stable cell lines expressing dCAS9-KRAB were generated. A lentiviral mediated integration system was used to stably express dCAS9-KRAB/guide RNAs in MCF10AT1 and MCF10CA1a cells. Virus production for Lentiviruses expressing dCas9 or guides is explained below (Figure 7). HEK-293-FT cells were plated in 100 mm plates at $2x10^6$ cells/plate. After 24 hours, cells were transfected with 10 μg TRE-dCAS9-KRAB, or guide RNAs, an enveloping plasmid PMD2-G, and a packaging plasmid pSPAX2 at a 2:1:1 ratio. DNA and X-tremeGENE (Sigma-Aldrich) were mixed in a 1:1 ratio and incubated at room temperature for 30 minutes in serum free medium. The DNA/X-tremeGENE solution was then added to the HEK-293-FT cells in 6 mL of complete medium. Cells were incubated 18 hours, and medium was removed. Ten milliliters of fresh complete media was added and virus collected after 24 and 48 hours. pLenti CMV-GFP 736-1 was used as a control to visualize the efficiency of the transfection. Lentivirus was concentrated to 10X using Lenti-X™ Concentrator Protocol (Clontech).

Next, MCF10AT1 and MCF10CA1a were plated at $5x10^5$ cells per well in a 6-well plate. The next day, 150 μL concentrated dCas9-KRAB virus was added to the cells along with 4μg/mL polybrene. After 24 hours, medium was changed to G418 (Sigma-Aldrich #4727878001) containing medium at a concentration of 1500 μg/mL (http://cell-lines.toku-e.com/Antibiotics_14.html). Medium was changed every 3-4 days for three weeks until cells began to grow in colonies. These cells were harvested and induced for

dcas9 expression by induction every 24 hours with 1.5 μg/mL doxycycline for 24, 48, and 72 hours total (Figure 6). Samples were prepared in lysis buffer (see below), run in an 8.5% acrylamide gel, and stained overnight in Runx2 (1:1000; Cell Signaling). To detect dCas9, a 6% acrylamide gel was used, with overnight transfer at 30 Volts and overnight anti-CRISPR (Cas9) (1:1000; BioLegend, 844301).

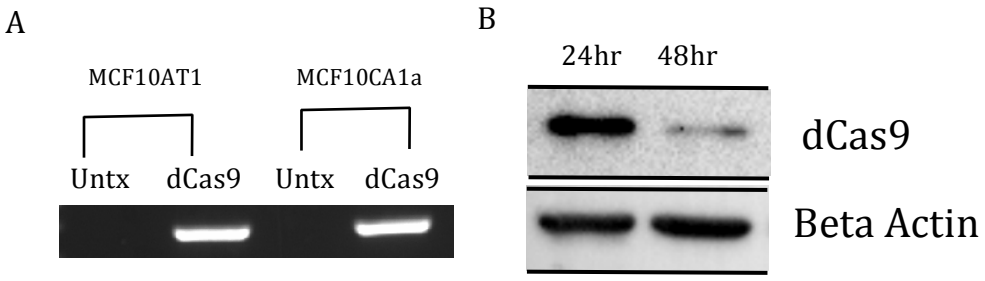

Figure 6: Incorporation and inducibility of dCas9 in MCF10AT1 and MCF10CA1a. A. Nested PCR of neomycin to check for incorporation of dCAS9 plasmid into the genome. **B.** Western blot of dCas9 expression after induction with doxycycline at hour 0.

After checking for dCas9 integration and induction using the primers forward primer Neo F-CGTTGGCTACCCGTGATATT and the reverse primer WPRE R-CATAGCGTAAAAGGAGCAACA for nested PCR (Figure 6), dCas9 expressing MCF10AT1 and MCF10CA1a were transduced with guide RNAs for promoter 1, promoter 2, and promoters 1 and 2 together. Infected cells were selected after 24 hours using 0.5/1 μg/mL and 2 μg/mL puromycin for MCF10CA1a and MCF10AT1, respectively. After 48 hours, puromycin was removed.

Guide at promoter 1

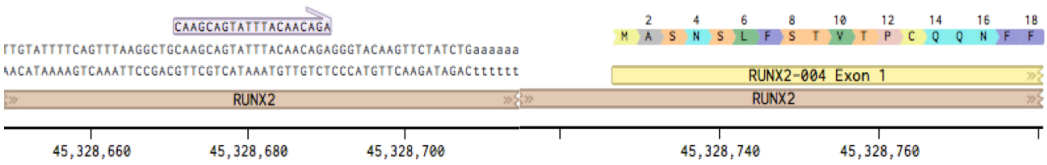

Guide at promoter 2

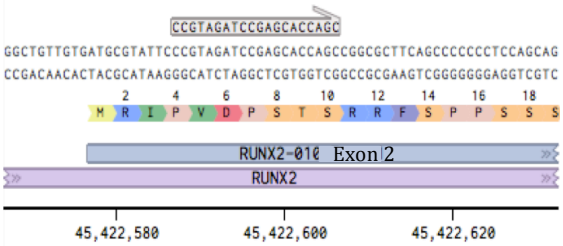

Figure 7: Genomic position of Guide RNAs to target Runx2 gene. The guide at promoter 1 binds to the region of the gene just before Exon 1, and the guide at promoter 2 binds at the beginning of Exon 2.

2.5 RNA Extraction and cDNA preparation

Once cells reached confluence, cells were scraped off a 100 mm plate and the cell pellets were stored at -80 °C until RNA extraction. RNA was extracted from pelleted cells using the Qiagen RNeasy Plus Mini Kit according to the manufacture's protocol. RNA was stored at -80 °C until cDNA was made using SuperScript III First Strand Synthesis System for RT-PCR (Invitrogen). RNA samples were sent to the UVM Advanced Genome Technologies Core for RNA quality analysis (Figure 8). RNA samples with RNA integrity numbers between 9.8 and 10 were used to generate cDNA.

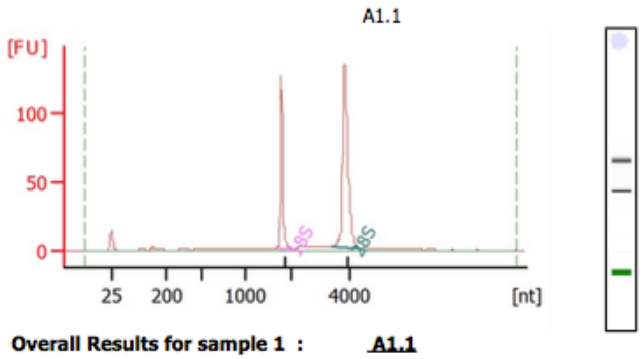

Overall Results for sample 1 : A1.1

RNA Area:	352.8
RNA Concentration:	344 ng/µl
rRNA Ratio [28s / 18s]:	2.0
RNA Integrity Number (RIN):	10 (B.02.08, Anomaly Threshold(s) manually adapted)
Result Flagging Color:	
Result Flagging Label:	RIN:10

Fragment table for sample 1 : A1.1

Name	Start Size [nt]	End Size [nt]	Area	% of total Area
18S	1,745	2,091	94.9	26.9
28S	3,384	4,498	193.7	54.9

Figure 8: RNA Integrity Example. RNA integrity number (RIN) is 10, which is the best score.

2.6 Quantitative Real-Time Polymerase Chain Reaction (q-RT-PCR)

cDNA was made as described above. SYBR green (BioRad) was used along with the following primers:

Table 1: Primer Sequences used in qPCR

Primer	Forward Primer sequence 5'-3'	Reverse Primer Sequence 5'-3'
hGAPDH	ATGTTCGTCATGGGTGTGAA	TGTGGTCATGAGTCCTTCCA
hRunx2	CAGCCCCAACTTCCTGTG	CCGGAGCTCAGCAGAATAAT
hRunx1	GTCGAAGTGGAAGAGGGAAA	CCGATGTCTTCGAGGTTCTC
hVEGF	CCTTGCTGCTCTACCTCCAC	CCATGAACTTCACCACTTCG
hIL-8	GTGCAGTTTTGCCAAGGAGT	CTCTGCACCCAGTTTTCCTT
hVimentin	GACGCCATCAACACCGAGTT	CTTTGTCGTTGGTTAGCTGGT
hE-cadherin	CGAGAGCTACACGTTCACGG	GGGTGTCGAGGGAAAAATAGG

hN-cadherin	TGCGGTACAGTGTAACTGGG	GAAACCGGGCTATCTGCTCG
hFibronectin	CGGTGGCTGTCAGTCAAAG	AAACCTCGGCTTCCTCCATAA
hITGA3	TGTGGCTTGGAGTGACTGTG	TCATTGCCTCGCACGTAGC
hITGB1	CCTACTTCTGCACGATGTGATG	CCTTTGCTACGGTTGGTTACATT
hSurvivin	AGGACCACCGCATCTCTACAT	AAGTCTGGCTCGTTCTCAGTG

q-RT-PCR was performed using Viia 7 Thermal cycler from Applied Biosystems (Life Technologies). The thermal cycling protocol was performed using a fast block, with denaturation at 95°C for 1 sec and annealing/extension at 60°C for 20 sec for 40 cycles. The melting curve analysis and polymerase activation and DNA denaturation were carried out at 95°C for 1 sec, 60°C for 1 min, and 95°C for 15 sec. Calculations were based on normalization to the control, GAPDH, and then again to the EV, giving delta delta threshold cycle (ddCT) values. Based on dCT values, the relative expression was calculated along with the positive and negative difference for error. All experiments were carried out on three independent biological replicates, with three technical replicates each. Statistical analysis was performed using a two-tailed, paired T-test.

2.7 Western Blotting

Protein isolation was done using direct lysis buffer. Cells were harvested via scraping or trypsinization from 100 mm plates when they reached 90% confluence. Direct lysis buffer containing 2 M urea, 10 mM DTT, 10% glycerol, 1M Tris-HCL pH 6.8, 2% SDS, 1 mg bromophenol blue, 250 μL protease inhibitor (Roche Diagnostics), and 5 μL MG132 protease inhibitor (Calbiochem) was added to cell pellets. Samples were boiled for 10 minutes at 100°C and then centrifuged at 21,000 x g for 2 minutes.

The protein lysates were loaded on an 8.5% acrylamide gel and run at 80 V for 20 minutes and 120 V for 1 hour. Transfer buffer (25 mM Tris, 192 mM glycine, 20% methanol, and water) was used with a submerged wet transfer system (BioRad) and performed at constant 300 mAmps for 2 hours. The PVDF membrane was incubated for one hour at room temperature in 5% milk/tris buffered saline (TBS), then in primary antibody in 5% milk/TBS at 4°C overnight, or for 30 minutes at room temperature, depending on the antibody. Membranes were washed with TBST for 20, 10, 10, 10 minutes before the appropriate secondary antibody was added at 1:2000 in 5% milk/TBS with 0.1% Tween for one hour at room temperature. Membranes were washed 10, 10, 10, 5 minutes before a 1-minute detection with Clarity Western ECL Substrate (Biorad). Antibodies used: Runx2 (Cell Signaling) at 1:1000, B-actin (Cell Signaling) at 1:3000, Runx1 (Cell Signaling) at 1:1000, E-cadherin (Cell Signaling) at 1:1000, N-cadherin (Cell Signaling) at 1:1000, and Vimentin (Santa Cruz Biotechnology) at 1:1000. Western Blots were quantified using Image Lab Software (Biorad) densitometry tool.

2.8 Cellular Characterization with Functional Assays

2.8.1 Cell Proliferation Assay

Proliferation assays are useful in determining cell proliferation rate (Vander Heiden, Cantley, & Thompson, 2009). When cells become cancerous, the proliferation rate often increases substantially because genes are upregulated that promote the constitutive uptake and metabolism of nutrients (Vander Heiden et al., 2009). We wanted to understand if knocking down Runx2 changed the proliferation rate in our cells.

Cells were plated on a 6-well plate at 35,000 cells per well, in triplicate. Cells were counted daily for four days. Untreated, shRUNX2, and EV cells were counted for both MCF10CA1a and MCF10AT1 from three independent infections.

2.8.2 Wound Healing (Scratch) Cell Motility Assay

A wound healing assay by making a scratch on a confluent cell culture plate is an inexpensive and simple assay to measure cell migration/motility (C. C. Liang, Park, & Guan, 2007). Cells are grown to confluence in monolayer culture before a scratch is made and images are captured at regular time points. This method is advantageous because it mimics migration *in vivo* to some extent (P. Liang, Averboukh, Keyomarsi, Sager, & Pardee, 1992). Cells were plated at $0.5x10^6$ cells/well (MCF10CA1a), and $0.3X10^6$ cells/well (MCF10AT1). After 48 hours, a scratch was made with a sterile 10 μL pipette tip. Complete media was replaced with serum-free media, to inhibit cell growth. Scratched area was then imaged by phase contrast microscopy. The scratch closure was imaged at 3, 6, 9, 12, and 26 hours in cells expressing either EV or shRunx2.

2.8.3 Cell Migration and Invasion

Cellular migration and invasion properties were examined to measure the effects of Runx2 knockdown in both MCF10AT1 and MCF10CA1a cells. Corning® BioCoat™ Matrigel® Invasion Chambers and Control Inserts, 24-Well, 8.0 micron, plates were used for this assay. Matrigel is a 3D gel basement membrane-like extract that supports morphogenesis, differentiation, and tumor growth (Kleinman & Martin, 2005). Matrigel invasion chambers were thawed to room temperature, rehydrated for two hours in

DMEM and 0.1% BSA before cells were plated in the insert at 50,000 cells/insert in DMEM and 0.1% BSA. Chemoattractant (complete media, as described above) was added to the well, outside the insert. After 18-24 hours, cells inside the chamber were removed by scraping with cotton-tipped applicators, inserts were washed in PBS, then fixed with ice cold methanol for 20 minutes, allowed to air dry for 30 minutes, stained with crystal violet for 20 minutes, and imaged using a Leica M165FC dissecting microscope equipped with a color camera.

2.9 Next Generation RNA Sequencing

Next-generation RNA sequencing is a recent development that has improved gene expression studies. Sequence-based methods for analysis of the global transcriptome have allowed alternative splicing isoforms to be identified, transcript fusions to be detected, as well as the identification of strand specific expression (Dillies et al., 2013). It can also be used to detect differential expression of genes between different tissues or conditions. It is ideal for detection of low expressing genes and can cover the entire transcribed portion of the genome (Dillies et al., 2013; Morozova & Marra, 2008). Next generation sequencing provides genome-wide information of the levels of gene expression, structure of the gene loci, and any sequence variation that is present (Morozova & Marra, 2008). This is a more precise and comprehensive alternative to microarrays and Sanger sequencing. Microarrays are a hybridization-based method that is not capable of fully examining a genome due to the many types and levels of RNA (Ozsolak & Milos, 2011). Next generation RNA sequencing does have limitations, especially for certain applications such as single strand transcription analysis, as strand switching may occur

during cDNA synthesis. Other biases may occur such as transcript-length bias, and biases at steps such as priming with random hexamers, ligations, or cDNA synthesis (Ozsolak & Milos, 2011).

RNA was isolated as described above. We used the TruSeq Stranded Total RNA Library Prep kit with Ribo-Zero Gold (Illumina, San Diego, CA, USA) to create the RNA library used for sequencing at the University of Vermont Advanced Genome Technologies Core Facilities Massively Parallel Sequencing Facility to sequence RNA samples infected with EV or shRunx2 in both MCF10AT1 and MCF10CA1a. Next, using the Kappa Real-Time Library Amplification Kit (Kapa Biosystems, Wilmington, MA, USA) DNA was amplified further. The library was quantified using the Qubit dsDNA HS Assay Kit (Thermo Fischer Scientific) and analyzed using Bio-analyzer (Agilent Technologies, Santa Clara, CA, USA) before being sequenced as single-end 100 bp reads (IlluminaHiSeq1000, UVM Advanced Genome Technologies Core). Sequence files (fastq) were mapped to the most recent human genome assembly (hg38) (PMID: 23104886). Expression counts were determined by HTSeq using gene annotations (Gencode v25) and differential expression by DESeq2. Data was then assessed by principle component analysis.

CHAPTER 3: RESULTS

3.1 Runx2 levels can be decreased by both shRNA and CRISPRi methods

Runx2 levels were measured using qPCR as well as Western blot to validate shRNA lentiviral knockdown of Runx2. Figure 9 demonstrates by qPCR that in MCF10CA1a and MCF10AT1 cells Runx2 levels post-sort were depleted by 50%, *p= 0.001804 and 80%, *p=0.018803, respectively. Western blot densitometry analysis shows that Runx2 was reduced about 60% in both MCF10AT1 and MCF10CA1a, *p=0.008, and *p=0.0046, respectively. Runx1 levels were also measured because Runx1 and Runx2 have been reported to have a reciprocal relationship in MDA-MB-231 and MCF7 breast cancer cell lines (Cohen-Solal, Boregowda, & Lasfar, 2015). However, analysis of Runx1 at both RNA and protein levels in cells with shRunx2 showed no significant difference upon depletion of Runx2 in this cell model. We observed significant knockdown of Runx2 on both RNA and protein levels in the shRUNX2 cells compared to EV cells in MCF10AT1 and MCF10CA1a (Figure 9).

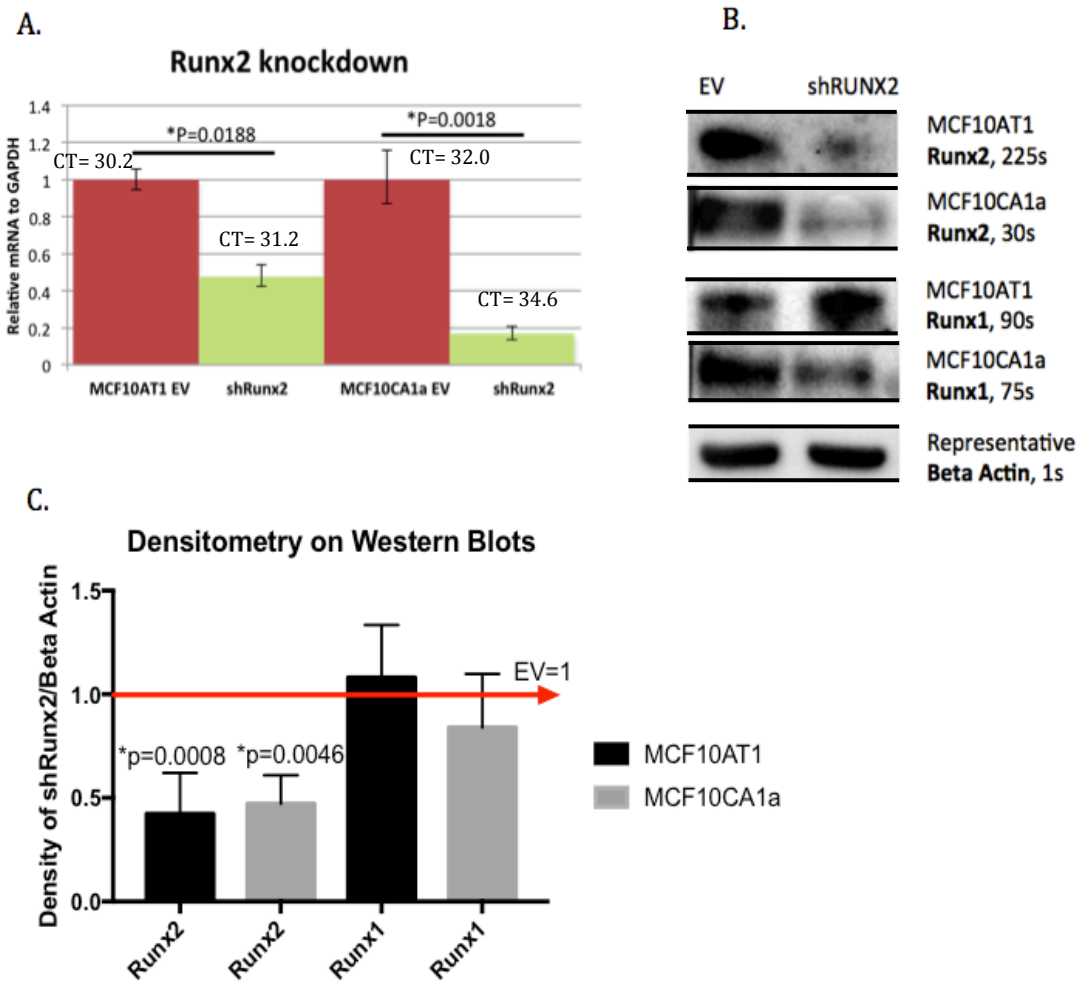

Figure 9: Validation of Runx2 knockdown in MCF10AT1 and MCF10CA1a using shRNA A. Knockdown Runx2 mRNA in MCF10AT1 and MCF10CA1a shRunx2 versus empty vector cells. Paired, two-tailed *t* test *p value <0.05, **p <0.01 for empty vector versus shrunx2. CT= Threshold cycle. **B.** Western blot of Runx2 and Runx1 expression in empty vector versus shRunx2 MCF10AT1 and MCF10CA1a. **C.** Densitometry of Runx2 and Runx1 protein expression from Western blots, n=5, *p <0.01.

3.2 Runx2 knockdown decreases the expression of mesenchymal markers in premalignant MCF10AT1 cells

We tested the hypothesis that Runx2 knockdown decreased mesenchymal properties of the cells, while increasing epithelial characteristics. Runx2 targets including Vimentin, N-cadherin, E-cadherin, Fibronectin, VEGF, and IL-8 were identified to study the effect on molecular markers of EMT (Pratap et al., 2009; Pratap et al., 2006; Pratap et al., 2008). Other targets, including Survivin, ITGB1, and ITGA3, were chosen from RNA sequencing datasets based on their involvement in avoiding apoptosis and cell-to-cell contact. Expression levels of EMT markers including the epithelial marker E-Cadherin, and the mesenchymal markers N-Cadherin, Fibronectin, ITGA3, ITGB1, and Vimentin were measured (Figure 10). Although not statistically significant, there is a general trend towards decreased RNA expression of mesenchymal markers. The epithelial marker, E-cadherin, as well as the two integrins, did not change. Since integrins are secreted proteins, their secreted levels may have changed, but overall RNA levels did not. Western blot densitometry to evaluate protein levels showed that the epithelial marker E-Cadherin does not change, while there is a slight decrease in both mesenchymal markers, N-Cadherin and Vimentin.

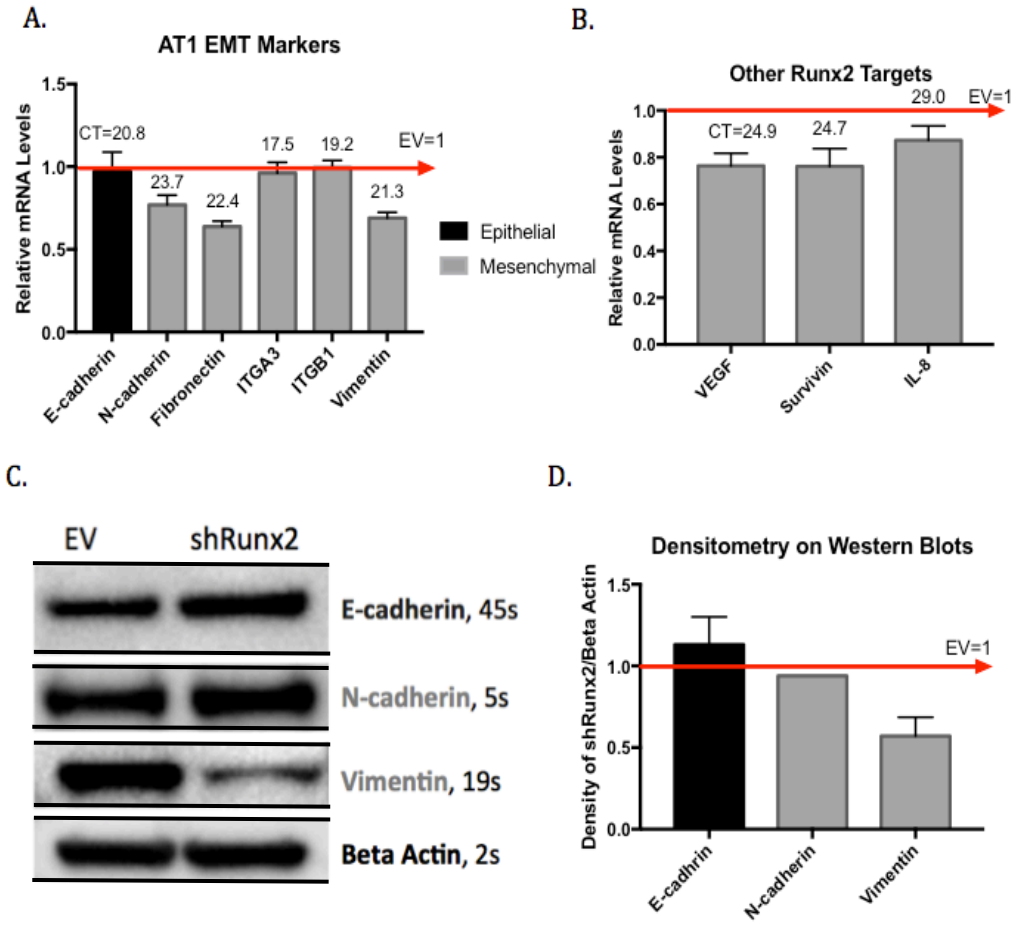

Figure 10: Decreased expression of EMT markers due to Runx2 knockdown in MCF10AT1. A. qPCR showing the expression levels of various epithelial and mesenchymal markers. **B.** Other Runx2 targets that contribute to EMT also decreased in response to Runx2 knockdown. **C.** Western blot of some epithelial and mesenchymal proteins. **D.** Densitometry of Western blots.

3.3 Proliferation rate is not affected by knockdown of Runx2 in MCF10AT1

Previous studies have shown that in various late-stage breast cancer cell lines, knockdown of Runx2 decreases tumor-forming capabilities (Pratap et al., 2009). We decided to test whether tumor-related proliferation characteristics were inhibited by Runx2 knockdown in both MCF10AT1 and MCF10CA1a cell lines. In MCF10AT1,

there was not a significant difference in proliferation rates between EV and shRunx2 cells (Figure 11). Although untreated MCF10AT1 parental cells showed slightly slower proliferation rates than the EV and shRunx2 cells, it was not statistically significant.

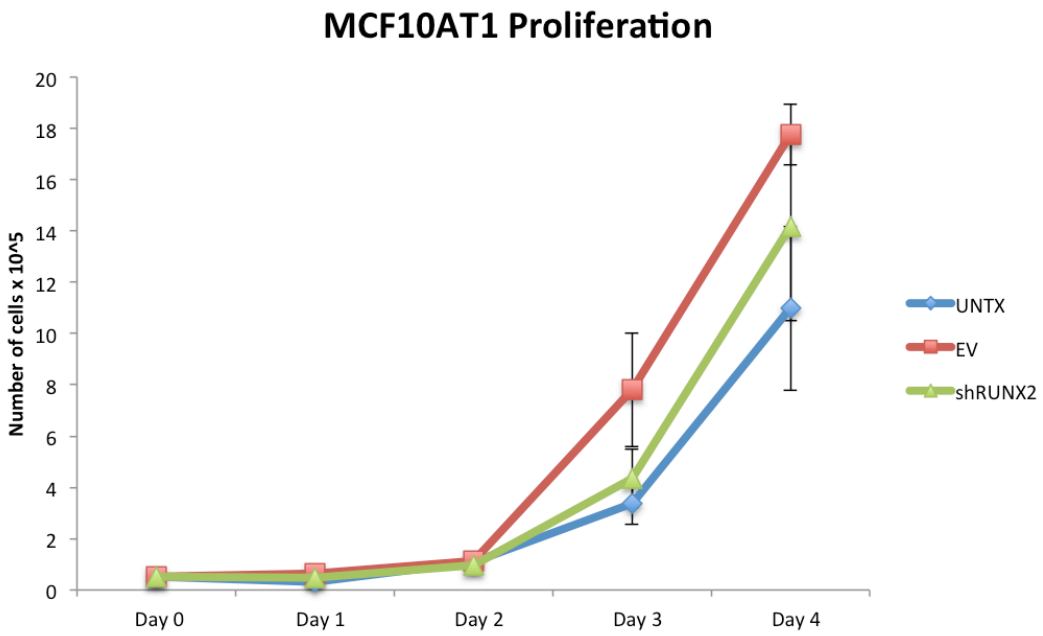

Figure 11: Proliferation rate in MCF10AT1 is not affected by Runx2 knockdown. $p > 0.05$. This is based on three biological replicates, counted in triplicate for four days.

3.4 Migration as measured by a scratch assay is not affected by Runx2 knockdown

Migration is an important step in metastasis because cancer cells must be able to sense and respond to chemical signals to lead them to a suitable environment in which to grow (Kozlow & Guise, 2005). One property of cancer cells is increased migration capabilities, leading to increased tumorigenesis. In the parental MCF10A cell lines, overexpression of Runx2 activates migration and invasion pathways through matrix

metalloprotease (MMP)-2, MMP-9, and osteopontin (Pratap et al., 2009). As described by Pratap et al., 2009, knockdown of Runx2 in triple-negative breast cancer cells abrogates a tumor phenotype. We investigated effects of Runx2 knockdown on cell migration in the MCF10AT1 and MCF10CA1a cell lines that represent premalignant and metastatic breast cancer cells derived from MCF10A cells. Runx2 knockdown did not appear to affect migration rate in MCF10AT1 (Figure 12).

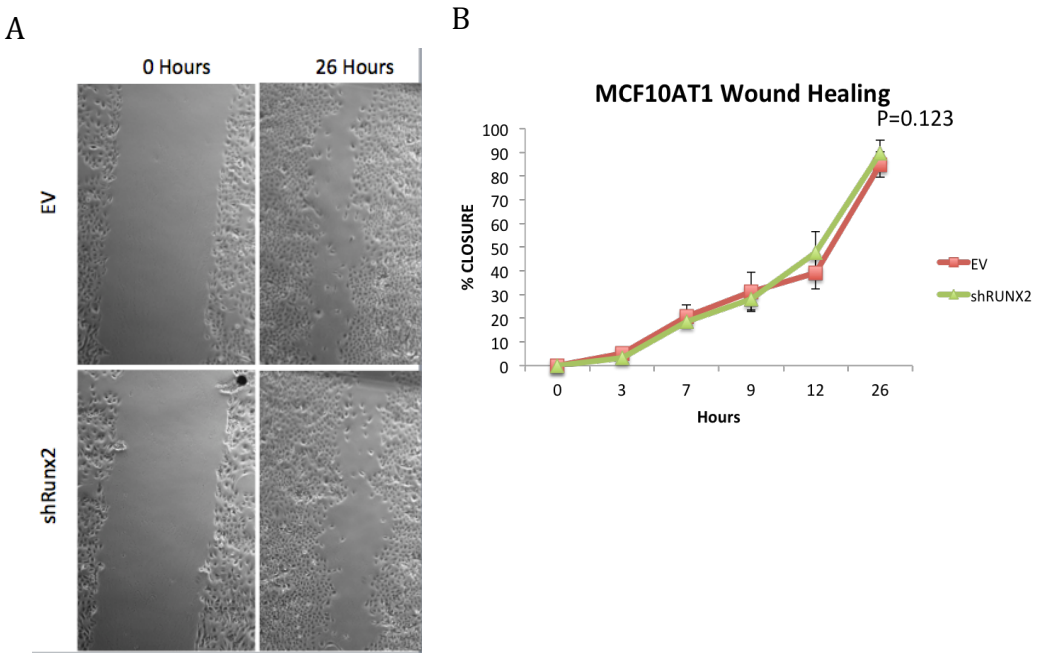

Figure 12: Runx2 knockdown does not affect cell migration in MCF10AT1. A. Representative images of scratch closure in EV versus shRunx2 at 0 and 26 hours after the scratch was made **B.** Graph showing percent closure of the scratch over time for both EV and shRunx2 MCF10AT1 cells, completed in three biological replicates, in triplicate.

3.5 Migration and invasion as measured by a Matrigel assay were not affected in MCF10AT1 when Runx2 was depleted

We measured both migration and invasion by using the Corning Matrigel Transwell Assay. These come with Matrigel coated inserts and non-Matrigel coated, or control inserts. The control inserts consist of a wire mesh that allows cells to demonstrate their migration capabilities. The Matrigel insert has the same mesh, but also a layer of Matrigel, which is used to measure invasion capabilities. Since Runx2 is known to upregulate genes involved in migration and invasion (Pratap et al., 2009), we assessed migration and invasion capabilities of Runx2 knockdown compared to EV cells. Runx2 knockdown did not alter either migration or invasion (Figure 13) in MCF10AT1 cells.

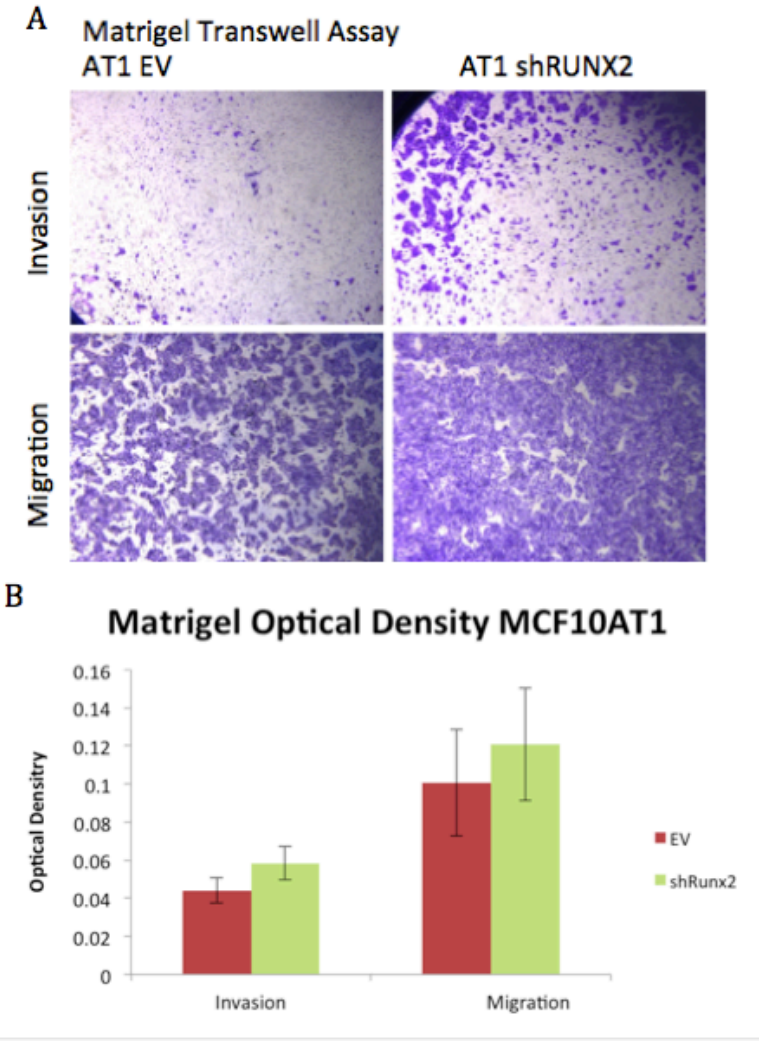

Figure 13: Runx2 knockdown does not alter migration and invasion capabilities in MCF10AT1. A. Representative images of invasion and migration chambers in the Matrigel Transwell Assay. **B.** Optical density of n=3 biological replicates for invasion and migration in both EV and shRunx2, $p>0.05$.

3.6 Runx2 knockdown affects the expression of both mesenchymal and epithelial markers in MCF10CA1a

Runx2 is a transcription factor for various genes involved in EMT. We measured the levels of some of the genes associated with EMT in response to Runx2 knockdown to determine if Runx2 influenced the expression of these genes directly. In the MCF10CA1a cells, the epithelial marker, E-cadherin, and the mesenchymal markers, N-cadherin, fibronectin, ITGA3, ITGB1, and vimentin, decreased by qPCR. We also measured the protein levels using Western blot, which confirms the qPCR results. E-cadherin protein levels decreased significantly as shown by Western blot densitometry (Figure 14) when Runx2 knockdown occurs. However, the changes in vimentin and N-cadherin between EV and shRunx2 are not significantly altered on protein levels (Figure 14).

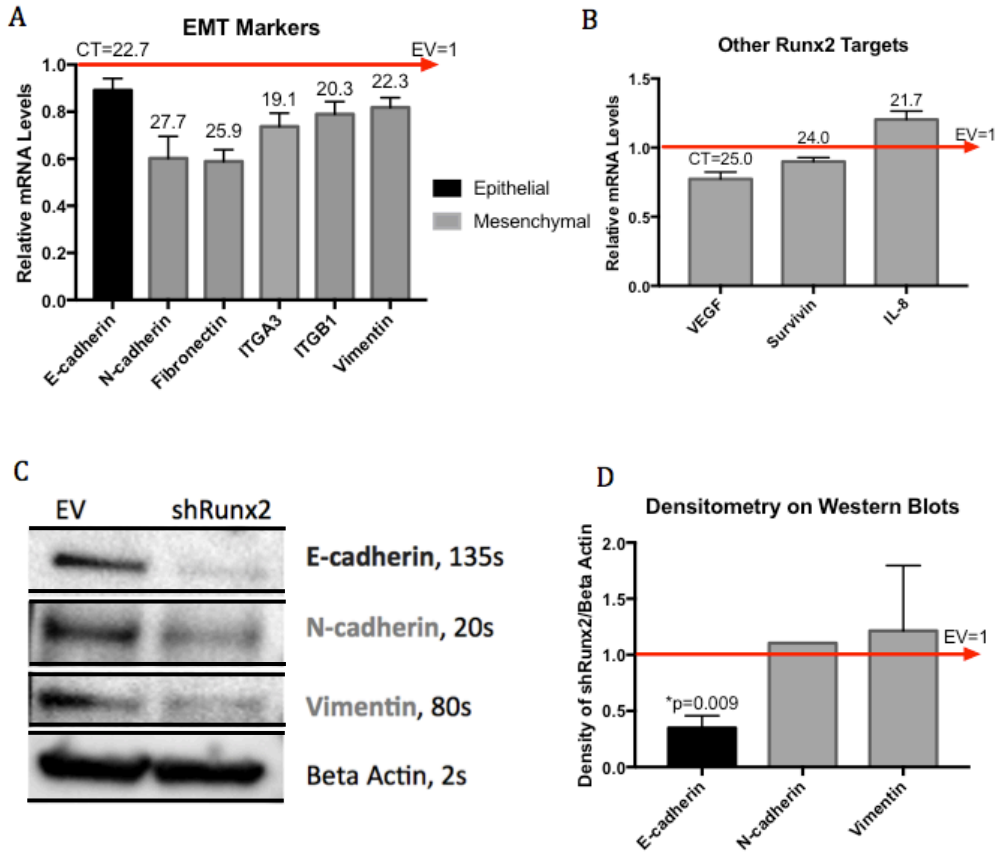

Figure 14: Runx2 knockdown changes expression level of Runx2 target genes in MCF10CA1a. A. qPCR of epithelial and mesenchymal markers shows a general decrease in expression levels in shRunx2 cells compared to EV, paired, two-tailed *t* test, p>0.05. **B.** Additional Runx2 target gene expression levels measured by qPCR. **C.** Representative Western blots of an epithelial and two mesenchymal markers. **D.** Densitometry on Western blots. For E-cadherin, n=5 and *p <0.01.

3.7 Runx2 knockdown did not change the proliferation rate in MCF10CA1a

To determine if knocking down Runx2, a tumor promoter, affects proliferation, MCF10CA1a cells were counted daily for four days to determine proliferation rate. There was no significant difference between proliferation rates of empty vector and shRunx2 expressing cells in MCF10CA1a (Figure 15).

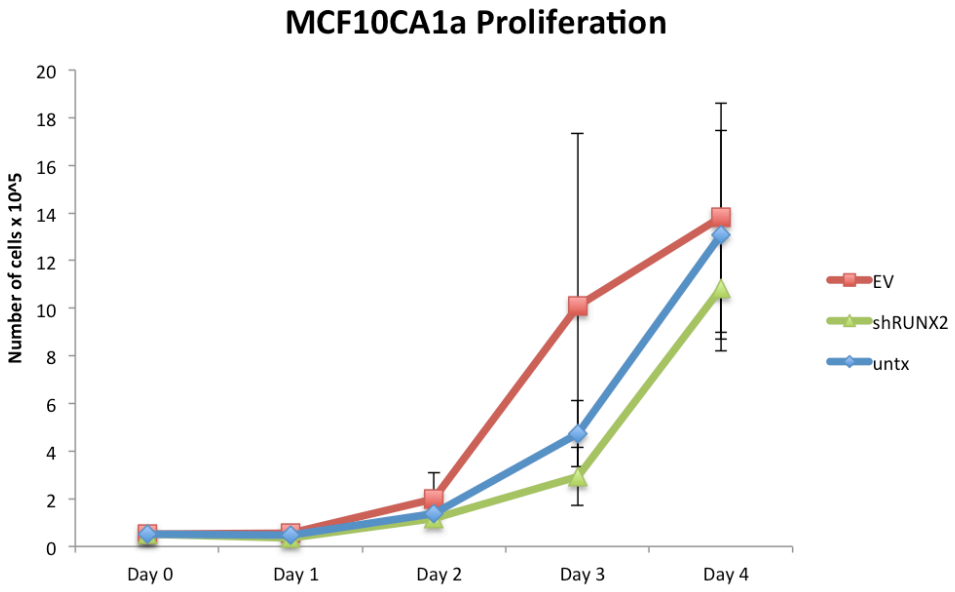

Figure 15: Runx2 knockdown does not affect MCF10CA1a proliferation rates. p >>0.05, three biological replicates, each counted in triplicate.

3.8 Migration rate is slightly increased by Runx2 knockdown in MCF10CA1a

The migration rate as measured by scratch assays was determined to evaluate the effect of Runx2 knockdown on migration properties of MCF10CA1a cells, since it decreased various proteins involved in the epithelial to mesenchymal transition. Although not significant (p=0.078), Runx2 knockdown marginally increased the migration rate of shRunx2 cells compared to EV, as measured by percent closure of scratches (Figure 16).

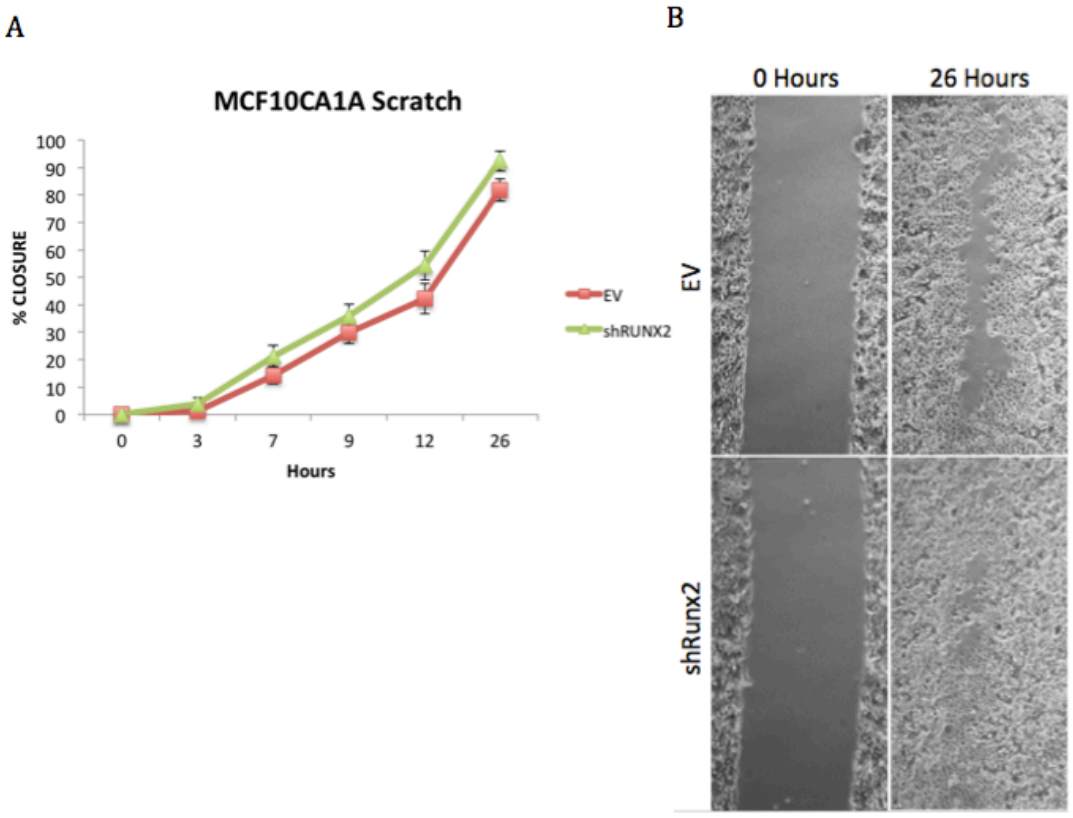

Figure 16: Runx2 knockdown slightly alters migration rate in MCF10CA1a. A. Percent closure over time in the EV versus shRunx2 MCF10CA1a cells, p=0.078, n=6 from three biological replicates. **B.** Representative images of scratches at 0 hours and 26 hours in EV and shRunx2.

3.9 Migration and invasion capabilities are not altered by Runx2 knockdown in MCF10CA1a

As Runx2 is a tumor promoter, knocking down Runx2 may alter the ability of these cells to migrate and invade. Although Runx2 knockdown decreased the expression of various mesenchymal genes involved in EMT on an RNA level, migration and invasion properties of these cells as measured by Matrigel Transwell Assay were not affected (Figure 17).

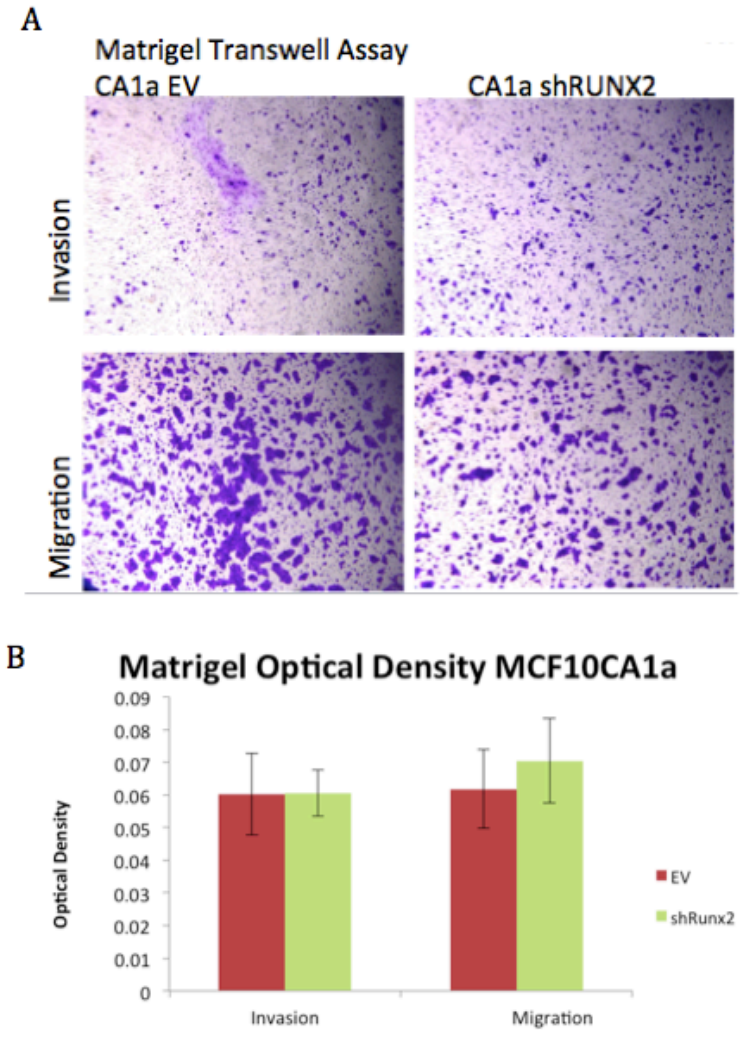

Figure 17: Runx2 knockdown does not alter migration and invasion capabilities in MCF10CA1a. A. Representative images of the invasion and migration Matrigel Transwell Assays in EV and shRunx2. **B.** Optical density from three biological replicates, $p > 0.05$.

3.10 Next Generation RNA sequencing analysis of EV and shRunx2 expressing cells

RNA sequencing can identify genes that are differentially expressed and may be contributing to a cell's cancer phenotype (Langmead, Hansen, & Leek, 2010; P. Liang et al., 1992). The identification of differentially expressed genes between the EV and shRunx2 cell lines can lead to the identification of novel pathways that may be regulated by Runx2. We encountered a few problems when completing the RNA sequencing analysis. Figure 18 is a Principal Component Analysis (PCA) plot of RNA sequencing datasets that shows variation in global RNA expression between samples, courtesy of Coralee Tye. The PCA analysis of our datasets from both MCF10AT1 and MCF10CA1a showed no significant changes in global RNA expression. This is a problem because the change in global RNA expression in shRunx2 cells should be significantly different than that in the EV cells. Further analysis using DEseq revealed no significantly changed RNAs between MCF10CA1a EV and shRunx2 expressing cells and only 25 differentially expressed RNAs between MCF10AT1 EV and shRunx2 expressing cells. To investigate this unexpected result, we included RNA sequencing data from untreated MCF10AT1 and MCF10CA1a cells and reanalyzed all datasets using PCA and reviewed RUNX2 RNA sequencing read counts between untreated, EV, and shRunx2 cells. Our data revealed that EV and shRunx2 expressing cells grouped closer to each other compared to the untreated cells by PCA analysis (Figure 18). Furthermore, EV expressing cells

seemed have Runx2 transcript levels similar to shRunx2 expressing cells (data not shown). Because of similar alterations in RUNX2 RNA levels in EV versus shRunx2 cells, further analysis was not possible. We think this discrepancy could be resolved in the future by using another EV or scramble shRNA as a control.

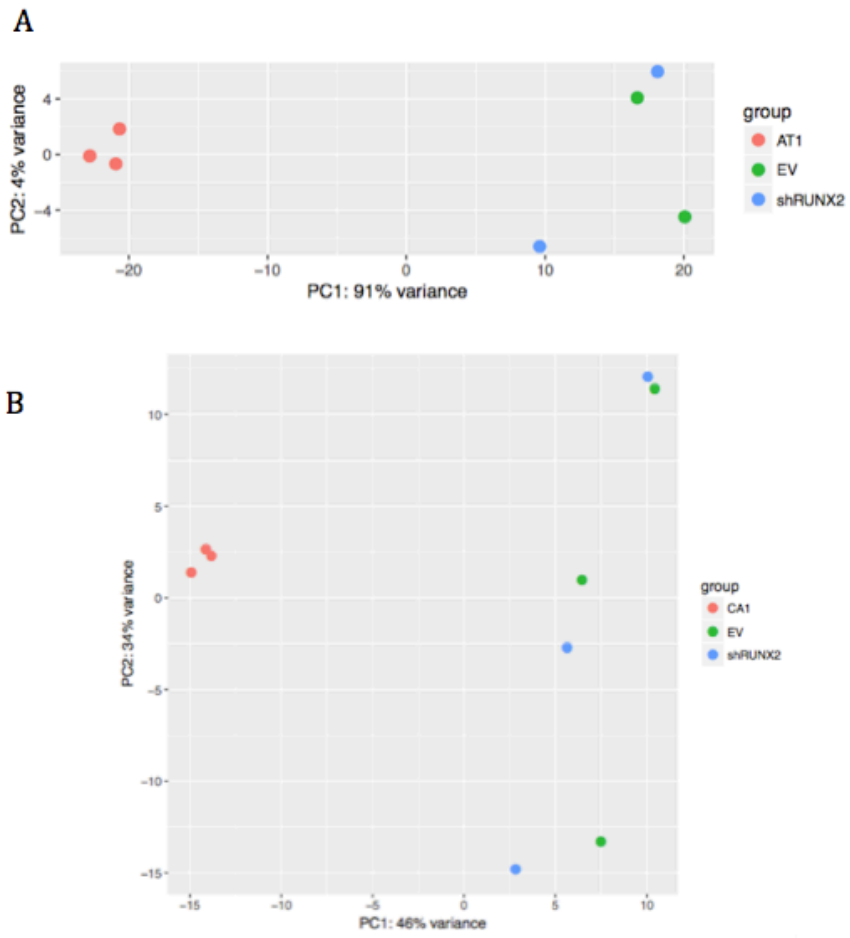

Figure 18: Principal Component Analysis (PCA) of RNA sequencing using next generation sequencing. A. PCA plot of global MCF10AT1 RNA sequencing data. **B.** PCA plot of global MCF10CA1a RNA sequencing data.

3.11 Inducible Knockdown of Runx2 using the CRISPRi system

We used an inducible CRISPRi system as an alternative method to knock down Runx2. First, MCF10AT1 and MCF10CA1a cells were transfected with dCas9-KRAB, a catalytically dead nickase. After selection with G418, cells were induced with doxycycline. dCas9 protein was detectable by Western blotting (Figure 6). Then, cells were infected with one or both guide RNAs designed to target Runx2 at promoter 1 and promoter 2. We tested whether the induction caused decreased Runx2 levels by Western blot (Figure 19).

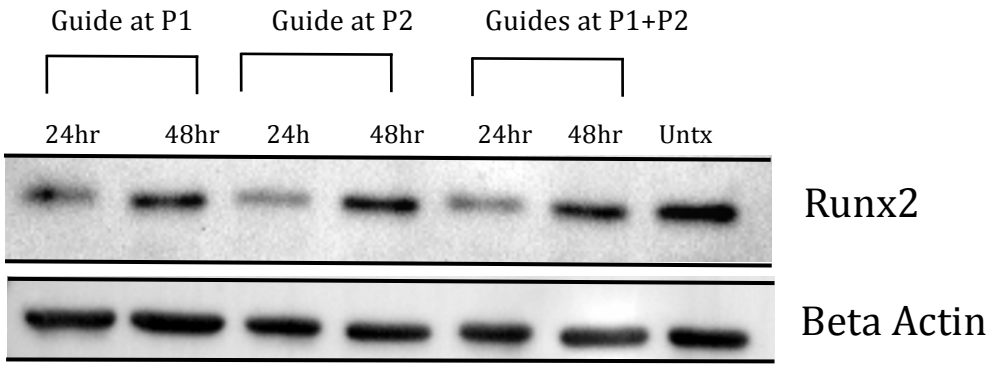

Figure 19: CRISPRi knockdown of Runx2. Western blot of Runx2 expression in dCas9/guide and untreated cells. Cells were induced at hour 0 with doxycycline and cultured for 24 and 48 hours.

CHAPTER 4: DISCUSSION

In this study, we show that Runx2 knockdown influences expression of genes involved in the epithelial to mesenchymal transition in both MCF10AT1 and MCF10CA1a. This is supported by qPCR and Western blot data showing that knockdown of Runx2 decreases the expression of N-cadherin, Fibronectin, and Vimentin. These genes are involved in making cancer cells more mesenchymal, which is an important step in the EMT process involved in metastasis. Supporting these observations, in normal mammary epithelial cells, aberrant Runx2 overexpression promotes EMT-like changes and disrupts normal breast epithelial structure (Akech et al., 2010). Additional Runx2 targets that may play a role in tumorigenesis are Survivin, IL-8, and VEGF. Survivin inhibits apoptosis and mitosis regulation, VEGF is involved in angiogenesis, and IL-8 is involved with initial colony growth as well as apoptosis resistance (Hartman et al., 2013; Span et al., 2004). Both Survivin and IL-8 decreased slightly in response to Runx2 knockdown. One other target we measured was PTHrP. PTHrP is involved in activating osteoclasts, which in turn, allows breast cancer cells to survive in bone (Boras-Granic & Wysolmerski, 2012). Runx2 activates genes such as PTHrP, making it an important mediator of interactions between bone and breast cancer cells when they metastasize to bone (Chen, Sosnoski, & Mastro, 2010). However, our results did not show a difference in PTHrP expression between EV and shRunx2 cells.

In addition to promoting a mesenchymal phenotype, overexpression of Runx2 in MCF10A cells causes an increase in proliferation and a loss of basement membrane formation compared to control (Pratap et al., 2009). To test if this was also true in our model, a proliferation assay was performed. In MCF10AT1 and MCF10CA1a,

knockdown of Runx2 did not seem to affect the proliferation rate significantly. MCF10CA1a shRunx2 cells proliferated slightly slow than EV cells, however the difference was not significant. One explanation for why these results contradict previous data that show Runx2 knockdown changes functional aspects of other breast cancer cell lines could be the effects of the EV in our system. In addition, the effect of RUNX2 knockdown has not been studied in this MCF10A progression series, where Runx2 levels are already low compared to other triple-negative breast cancer cell lines, such as MDA-MB-231. It is possible that levels are already too low, so knocking them down does not significantly affect functional characteristics of these cells.

Runx2 is known to directly mediate migration and invasion by activating MMPs and osteopontin in some cancer cell types (Akech et al., 2010). It also regulates the pro-angiogenic factor VEGF, indicating that Runx2 may have a role in promoting the early events in breast cancer (Akech et al., 2010). This raises the hypothesis that Runx2 knockdown may inhibit invasion and migration in these cells. Since the mesenchymal markers we tested decreased, and VEGF also decreased, we decided to test if migration of these cells was inhibited. Scratch migration assays are a useful way of measuring migration in a culture that mimics epithelial conditions (C. C. Liang et al., 2007). Another method of measuring both migration and invasion is to use the Matrigel chambers. Each Matrigel-coated chamber measures invasion. The more cells that can pass through the Matrigel matrix, the better ability they have to invade. Since knocking down Runx2 decreases levels of mesenchymal genes including N-cadherin, Vimentin, and Fibronectin, which help regulate the invasion and migration process, we expected that there would be less invasion and migration in the Runx2 knockdown cells. However,

there was not a difference between the EV and shRunx2 in MCF10AT1 or MCF10CA1a in terms of migration or invasion capabilities of these cells. Since these cells represent premalignant and metastatic cells with relatively low levels of Runx2, Runx2 regulation may be different than in the highly metastatic MDA-MB-231 cells.

We also investigated the effects of Runx2 knockdown on global RNA expression in both MCF10AT1 and MCF10CA1a using RNA sequencing. A relatively new application of RNA sequencing is the ability to quantify gene expression based on the number of mapped reads (Tarazona, Garcia-Alcalde, Dopazo, Ferrer, & Conesa, 2011). We hoped to identify differentially expressed genes between the EV and shRunx2 expressing MCF10AT1 cells, representative of a less aggressive cancer. These differentially expressed genes could be used to identify novel pathways controlled by Runx2 in cancer progression. However, due to non-specific effects observed in the EV control, our RNA sequencing data could not be analyzed further. In Figure 18, on the left hand side of the PCA plot, the three untreated replicates of the parental MCF10AT1 or MCF10CA1a cells cluster together very closely. We would expect that the EV expressing cells would group closer to the untreated cells than the shRNA cells. However, the EV and shRunx2 sample pairs grouped together in PCA, indicating variation between biological replicates. The other problem is the effect of the EV on Runx2 transcript levels that is almost comparable to that of shRunx2. This EV and shRNA were used in published data (Pratap et al., 2009), but in the MDA-MB-231 cells, where the effect of the EV was less drastic. However, in our system, EV effects prevented further analysis of the RNA sequencing data. A different empty vector or scramble shRNA control could be used to avoid this in the future.

We also developed an alternative method to knockdown Runx2 using CRISPRi. This method has advantages over shRNA-mediated knockdown because Runx2 knockdown can be modulated by an inducible system. This allows control over the level of Runx2 knockdown, and can be reversed if necessary. Future directions include characterization of the Runx2 knockdown in these cells. Since the effects of doxycycline seem to disappear by the 48 hour mark (Figure 19), dCas9/Guide cells were re-induced with doxycycline every 24 hours for up to 72 hours and show a time dependent decrease of Runx2 protein levels is possible (data not shown). Once the characterization of the Runx2 knockdown of these cells is complete, they can be used to repeat the functional assays to investigate the effects of Runx2 knockdown in the MCF10A series, without the limitation of the EV.

CHAPTER 5: CONCLUSION

Runx2 has been shown to play a role in promoting the early stages of breast cancer, as well as later, metastatic stages by changing the expression of various genes (Barnes et al., 2004; Pratap et al., 2009; Pratap et al., 2006). Our results indicate that Runx2 knockdown decreases the expression of various mesenchymal markers, such as N-cadherin, Fibronectin, and Vimentin in MCF10AT1 and MCF10CA1a breast cancer cells. However, we did not find a difference in functional characteristics or in RNA sequencing of EV versus shRunx2 cells, possibly due to nonspecific effects of EV on Runx2 levels. We need to reevaluate our data using a different EV control. Alternatively we could use other methods of Runx2 knockdown, such as CRISPRi dCas9 cells we developed against Runx2 that will allow investigation of the effects of Runx2 depletion on breast cancer progression.

CHAPTER 6: REFERENCES

Akech, J., Wixted, J. J., Bedard, K., van der Deen, M., Hussain, S., Guise, T. A., . . . Lian, J. B. (2010). Runx2 association with progression of prostate cancer in patients: mechanisms mediating bone osteolysis and osteoblastic metastatic lesions. *Oncogene, 29*(6), 811-821. doi:10.1038/onc.2009.389

Baniwal, S. K., Khalid, O., Gabet, Y., Shah, R. R., Purcell, D. J., Mav, D., . . . Frenkel, B. (2010). Runx2 transcriptome of prostate cancer cells: insights into invasiveness and bone metastasis. *Mol Cancer, 9*, 258. doi:10.1186/1476-4598-9-258

Barnes, G. L., Hebert, K. E., Kamal, M., Javed, A., Einhorn, T. A., Lian, J. B., . . . Gerstenfeld, L. C. (2004). Fidelity of Runx2 activity in breast cancer cells is required for the generation of metastases-associated osteolytic disease. *Cancer Res, 64*(13), 4506-4513. doi:10.1158/0008-5472.CAN-03-3851

Blyth, K., Cameron, E. R., & Neil, J. C. (2005). The RUNX genes: gain or loss of function in cancer. *Nat Rev Cancer, 5*(5), 376-387. doi:10.1038/nrc1607

Boras-Granic, K., & Wysolmerski, J. J. (2012). PTHrP and breast cancer: more than hypercalcemia and bone metastases. *Breast Cancer Res, 14*(2), 307. doi:10.1186/bcr3129

Chen, Y. C., Sosnoski, D. M., & Mastro, A. M. (2010). Breast cancer metastasis to the bone: mechanisms of bone loss. *Breast Cancer Res, 12*(6), 215. doi:10.1186/bcr2781

Chimge, N. O., & Frenkel, B. (2013). The RUNX family in breast cancer: relationships with estrogen signaling. *Oncogene, 32*(17), 2121-2130. doi:10.1038/onc.2012.328

Choi, J. Y., Pratap, J., Javed, A., Zaidi, S. K., Xing, L., Balint, E., . . . Stein, G. S. (2001). Subnuclear targeting of Runx/Cbfa/AML factors is essential for tissue-specific differentiation during embryonic development. *Proc Natl Acad Sci U S A, 98*(15), 8650-8655. doi:10.1073/pnas.151236498

Cohen-Solal, K. A., Boregowda, R. K., & Lasfar, A. (2015). RUNX2 and the PI3K/AKT axis reciprocal activation as a driving force for tumor progression. *Mol Cancer, 14*, 137. doi:10.1186/s12943-015-0404-3

Colditz, G. A. (1998). Relationship between estrogen levels, use of hormone replacement therapy, and breast cancer. *J Natl Cancer Inst, 90*(11), 814-823.

Dawson, P. J., Wolman, S. R., Tait, L., Heppner, G. H., & Miller, F. R. (1996). MCF10AT: a model for the evolution of cancer from proliferative breast disease. *Am J Pathol, 148*(1), 313-319.

DeSantis, C., Ma, J., Bryan, L., & Jemal, A. (2014). Breast cancer statistics, 2013. *CA Cancer J Clin, 64*(1), 52-62. doi:10.3322/caac.21203

Dillies, M. A., Rau, A., Aubert, J., Hennequet-Antier, C., Jeanmougin, M., Servant, N., . . . French StatOmique, C. (2013). A comprehensive evaluation of normalization methods for Illumina high-throughput RNA sequencing data analysis. *Brief Bioinform, 14*(6), 671-683. doi:10.1093/bib/bbs046

Gonzalez-Moreno, O., Lecanda, J., Green, J. E., Segura, V., Catena, R., Serrano, D., & Calvo, A. (2010). VEGF elicits epithelial-mesenchymal transition (EMT) in

prostate intraepithelial neoplasia (PIN)-like cells via an autocrine loop. *Exp Cell Res, 316*(4), 554-567. doi:10.1016/j.yexcr.2009.11.020
Guise, T. A. (2002). The vicious cycle of bone metastases. *J Musculoskelet Neuronal Interact, 2*(6), 570-572.
Hartman, Z. C., Poage, G. M., den Hollander, P., Tsimelzon, A., Hill, J., Panupinthu, N., . . . Brown, P. H. (2013). Growth of triple-negative breast cancer cells relies upon coordinate autocrine expression of the proinflammatory cytokines IL-6 and IL-8. *Cancer Res, 73*(11), 3470-3480. doi:10.1158/0008-5472.CAN-12-4524-T
Herzenberg, L. A., Parks, D., Sahaf, B., Perez, O., Roederer, M., & Herzenberg, L. A. (2002). The history and future of the fluorescence activated cell sorter and flow cytometry: a view from Stanford. *Clin Chem, 48*(10), 1819-1827.
Hong, Deli., Messier, Terri L., Tye, Coralee E., Dobson, Jason R., Fritz, Andrew J., Sikora, Kenneth R., Browne, Gillian., Stein, Janet L., Lian, Jane B., and Stein, Gary S. (2017). Runx2 stabilizes the mammary epithelial cell phenotype and prevents epithelial to mesenchymal transition. *Oncotarget, 8*, 17610-17627. doi: 10.18632/oncotarget.15381
Ito, Y., Bae, S. C., & Chuang, L. S. (2015). The RUNX family: developmental regulators in cancer. *Nat Rev Cancer, 15*(2), 81-95. doi:10.1038/nrc3877
Kleinman, H. K., & Martin, G. R. (2005). Matrigel: basement membrane matrix with biological activity. *Semin Cancer Biol, 15*(5), 378-386. doi:10.1016/j.semcancer.2005.05.004
Kozlow, W., & Guise, T. A. (2005). Breast cancer metastasis to bone: mechanisms of osteolysis and implications for therapy. *J Mammary Gland Biol Neoplasia, 10*(2), 169-180. doi:10.1007/s10911-005-5399-8
Lamouille, S., Xu, J., & Derynck, R. (2014). Molecular mechanisms of epithelial-mesenchymal transition. *Nat Rev Mol Cell Biol, 15*(3), 178-196. doi:10.1038/nrm3758
Langmead, B., Hansen, K. D., & Leek, J. T. (2010). Cloud-scale RNA-sequencing differential expression analysis with Myrna. *Genome Biol, 11*(8), R83. doi:10.1186/gb-2010-11-8-r83
Larson, M. H., Gilbert, L. A., Wang, X., Lim, W. A., Weissman, J. S., & Qi, L. S. (2013). CRISPR interference (CRISPRi) for sequence-specific control of gene expression. *Nat Protoc, 8*(11), 2180-2196. doi:10.1038/nprot.2013.132
Levanon, D., & Groner, Y. (2004). Structure and regulated expression of mammalian RUNX genes. *Oncogene, 23*(24), 4211-4219. doi:10.1038/sj.onc.1207670
Liang, C. C., Park, A. Y., & Guan, J. L. (2007). In vitro scratch assay: a convenient and inexpensive method for analysis of cell migration in vitro. *Nat Protoc, 2*(2), 329-333. doi:10.1038/nprot.2007.30
Liang, P., Averboukh, L., Keyomarsi, K., Sager, R., & Pardee, A. B. (1992). Differential display and cloning of messenger RNAs from human breast cancer versus mammary epithelial cells. *Cancer Res, 52*(24), 6966-6968.
Mendez, M. G., Kojima, S., & Goldman, R. D. (2010). Vimentin induces changes in cell shape, motility, and adhesion during the epithelial to mesenchymal transition. *FASEB J, 24*(6), 1838-1851. doi:10.1096/fj.09-151639

Morozova, O., & Marra, M. A. (2008). Applications of next-generation sequencing technologies in functional genomics. *Genomics, 92*(5), 255-264. doi:10.1016/j.ygeno.2008.07.001

Owens, T. W., Rogers, R. L., Best, S. A., Ledger, A., Mooney, A. M., Ferguson, A., . . . Naylor, M. J. (2014). Runx2 is a novel regulator of mammary epithelial cell fate in development and breast cancer. *Cancer Res, 74*(18), 5277-5286. doi:10.1158/0008-5472.CAN-14-0053

Ozsolak, F., & Milos, P. M. (2011). RNA sequencing: advances, challenges and opportunities. *Nat Rev Genet, 12*(2), 87-98. doi:10.1038/nrg2934

Pratap, J., Imbalzano, K. M., Underwood, J. M., Cohet, N., Gokul, K., Akech, J., . . . Stein, G. S. (2009). Ectopic runx2 expression in mammary epithelial cells disrupts formation of normal acini structure: implications for breast cancer progression. *Cancer Res, 69*(17), 6807-6814. doi:10.1158/0008-5472.CAN-09-1471

Pratap, J., Javed, A., Languino, L. R., van Wijnen, A. J., Stein, J. L., Stein, G. S., & Lian, J. B. (2005). The Runx2 osteogenic transcription factor regulates matrix metalloproteinase 9 in bone metastatic cancer cells and controls cell invasion. *Mol Cell Biol, 25*(19), 8581-8591. doi:10.1128/MCB.25.19.8581-8591.2005

Pratap, J., Lian, J. B., Javed, A., Barnes, G. L., van Wijnen, A. J., Stein, J. L., & Stein, G. S. (2006). Regulatory roles of Runx2 in metastatic tumor and cancer cell interactions with bone. *Cancer Metastasis Rev, 25*(4), 589-600. doi:10.1007/s10555-006-9032-0

Pratap, J., Wixted, J. J., Gaur, T., Zaidi, S. K., Dobson, J., Gokul, K. D., . . . Lian, J. B. (2008). Runx2 transcriptional activation of Indian Hedgehog and a downstream bone metastatic pathway in breast cancer cells. *Cancer Res, 68*(19), 7795-7802. doi:10.1158/0008-5472.CAN-08-1078

Rubinson, D. A., Dillon, C. P., Kwiatkowski, A. V., Sievers, C., Yang, L., Kopinja, J., . . . Van Parijs, L. (2003). A lentivirus-based system to functionally silence genes in primary mammalian cells, stem cells and transgenic mice by RNA interference. *Nat Genet, 33*(3), 401-406. doi:10.1038/ng1117

Santner, S. J., Dawson, P. J., Tait, L., Soule, H. D., Eliason, J., Mohamed, A. N., . . . Miller, F. R. (2001). Malignant MCF10CA1 cell lines derived from premalignant human breast epithelial MCF10AT cells. *Breast Cancer Res Treat, 65*(2), 101-110.

So, Jae Young., Lee, Hong Jin., Kramata, Pavel., Minden, Audrey., and Suh, Nanjoo. (2014). Differential Expression of Key Signaling Proteins in MCF10 Cell Lines, a Human Breast Cancer Progression Model. Mol Cell Pharmacol., 4(1): 31–40.

Span, P. N., Sweep, F. C., Wiegerinck, E. T., Tjan-Heijnen, V. C., Manders, P., Beex, L. V., & de Kok, J. B. (2004). Survivin is an independent prognostic marker for risk stratification of breast cancer patients. *Clin Chem, 50*(11), 1986-1993. doi:10.1373/clinchem.2004.039149

Stewart, S. A., Dykxhoorn, D. M., Palliser, D., Mizuno, H., Yu, E. Y., An, D. S., . . . Novina, C. D. (2003). Lentivirus-delivered stable gene silencing by RNAi in primary cells. *RNA, 9*(4), 493-501.

Tarazona, S., Garcia-Alcalde, F., Dopazo, J., Ferrer, A., & Conesa, A. (2011). Differential expression in RNA-seq: a matter of depth. *Genome Res, 21*(12), 2213-2223. doi:10.1101/gr.124321.111

Taylor, M. A., Sossey-Alaoui, K., Thompson, C. L., Danielpour, D., & Schiemann, W. P. (2013). TGF-beta upregulates miR-181a expression to promote breast cancer metastasis. *J Clin Invest, 123*(1), 150-163. doi:10.1172/JCI64946

Van den Haute, C., Eggermont, K., Nuttin, B., Debyser, Z., & Baekelandt, V. (2003). Lentiviral vector-mediated delivery of short hairpin RNA results in persistent knockdown of gene expression in mouse brain. *Hum Gene Ther, 14*(18), 1799-1807. doi:10.1089/104303403322611809

Vander Heiden, M. G., Cantley, L. C., & Thompson, C. B. (2009). Understanding the Warburg effect: the metabolic requirements of cell proliferation. *Science, 324*(5930), 1029-1033. doi:10.1126/science.1160809

Vimalraj, S., Arumugam, B., Miranda, P. J., & Selvamurugan, N. (2015). Runx2: Structure, function, and phosphorylation in osteoblast differentiation. *Int J Biol Macromol, 78*, 202-208. doi:10.1016/j.ijbiomac.2015.04.008

Wiznerowicz, M., & Trono, D. (2003). Conditional suppression of cellular genes: lentivirus vector-mediated drug-inducible RNA interference. *J Virol, 77*(16), 8957-8961.